



Published in final edited form as:

*Chem Commun (Camb)*. 2017 December 07; 53(98): 13093–13112. doi:10.1039/c7cc06287g.

## Recent Development of Transition-Metal Photoredox-Catalysed Reactions of Carbonyl Derivatives

Katarzyna N. Lee<sup>a,b</sup> and Ming-Yu Ngai<sup>a,b</sup>

<sup>a</sup>Department of Chemistry, Stony Brook University, Stony Brook, New York, 11794-3400, USA

<sup>b</sup>Institute of Chemical Biology and Drug Discovery, Stony Brook University, Stony Brook, New York 11794-3400, USA

### Abstract

Single-electron reduction of C=O and C=N bonds of aldehydes, ketones, and imines results in the formation of ketyl and  $\alpha$ -aminoalkyl anion radicals, respectively. These reactive intermediates are characterized by an altered electronic character with respect to their parent molecules and undergo a diverse range of synthetically useful transformations, which are not available to even-electron species. This Review summarizes the reactions of ketyl and  $\alpha$ -aminyl radicals generated from carbonyl derivatives under transition-metal photoredox-catalysed conditions. We primarily focus on recent developments in the field, as well as give a brief overview of catalytic enantioselective transformations that provide means to achieve precise stereocontrol over the reactivity of ion radicals.

### Introduction

Aldehydes, ketones, and imines are important intermediates for the assembly of complex molecules. Conventional synthetic protocols usually take advantage of the strong electrostatic polarization of carbon-heteroatom double bond of carbonyl (C=O) and iminyl (C=N) groups, which places a partial positive charge at the carbon atom, rendering the atom electrophilic and thus susceptible to undergo a nucleophilic attack. Methods that alter this natural reactivity pattern of carbonyl derivatives and enable them to engage in carbon-carbon bond forming reactions with non-nucleophilic partners have provided a paradigm shift in organic synthesis.<sup>1, 2</sup> Among the strategies reported in the literature, the formation of ketyl radicals *via* single electron reduction of carbonyl derivatives has emerged as an appealing route to access a wide range of valuable molecular architectures.<sup>3</sup> However, a widespread application of ketyl radicals in synthesis has been hindered by (i) the highly negative reduction potential<sup>4</sup> of aldehydes ( $E_{1/2}^{\text{red}} = -1.93$  V vs. SCE for benzaldehyde),<sup>5</sup> ketones ( $E_{1/2}^{\text{red}} = -2.11$  V vs. SCE for acetophenone),<sup>5</sup> and imines ( $E_{1/2}^{\text{red}} = -1.91$  V vs. SCE for *N*-benzylideneaniline)<sup>5</sup> (Scheme 1) and (ii) the requirement to employ toxic, air- and moisture-sensitive reducing agents, and harsh reaction conditions to generate the ketyl and

Correspondence to: Ming-Yu Ngai.

‡Footnotes relating to the main text should appear here. These might include comments relevant to but not central to the matter under discussion, limited experimental and spectral data, and crystallographic data.

$\alpha$ -aminoalkyl anion radical intermediates. Accordingly, early examples of reductive coupling reactions between carbonyl derivatives and alkenes/alkynes were performed using very strong reductants such as alkali<sup>6</sup> and alkali earth<sup>7</sup> metals, tin,<sup>8-13</sup> zinc,<sup>14, 15</sup> titanium,<sup>16</sup> and samarium reagents,<sup>17-22</sup> as well as under electrochemical<sup>23-26</sup> and photochemical<sup>27-32</sup> conditions. Due to the severe drawbacks of these strategies, such as the requirement for a strong reductant and generation of a stoichiometric amount of organometallic by-products, there has been a growing demand for development of new methods to access ketyl and  $\alpha$ -aminoalkyl anion radicals under mild and eco-compatible reaction conditions. In order to address these issues, a number of reductive coupling reactions of carbonyl derivatives involving a catalytic amount of early transition (e.g., Ti, V) or lanthanide metals (e.g., Sm) have been developed over the years and applied in natural product synthesis.<sup>3, 33-38</sup> Nonetheless, complementary strategies to generate ketyl and  $\alpha$ -aminoalkyl anion radical intermediates and to harness their unusual reactivity are still highly sought after.

Over the past few decades, visible light photoredox catalysis has emerged as an attractive alternative to traditional ways of generating radical intermediates.<sup>39-43</sup> The use of photoredox catalysts, which, upon photoexcitation with visible light, can engage in single electron transfer (SET) processes with organic substrates, obviates the need for radical initiators and a stoichiometric amount of strong reducing agents. Since Ru<sup>II</sup>(bpy)<sub>3</sub>Cl<sub>2</sub> was first reported to engage in a SET with aromatic carbonyl compounds in the late 1970s,<sup>44</sup> visible light organometallic photoredox catalysis has become widely recognized as an efficient way to generate ketyl<sup>45-62</sup> and  $\alpha$ -aminoalkyl anion radicals under mild reaction conditions.<sup>58, 63-65</sup>

Since most of the photoexcited catalysts or the reduced forms thereof are not sufficiently reducing ( $E_{1/2}^{\text{red}} = -1.33$  V vs. SCE for Ru)<sup>66</sup> to reduce a carbonyl or iminyl species ( $E_{1/2}^{\text{red}} = -1.93$  V vs. SCE for benzaldehyde) (Scheme 1),<sup>5</sup> the majority of the reported examples of photoredox-catalysed formation of ketyl or  $\alpha$ -aminoalkyl anion radicals require Brønsted acids,<sup>49, 53, 54</sup> Lewis acids,<sup>47, 49, 50, 52, 55, 57, 62</sup> or acids generated *in situ*,<sup>56, 59-61</sup> as activators to promote the electron transfer step. With a Brønsted acid additive, proton-coupled electron transfer (PCET),<sup>67</sup> which involves a simultaneous transfer of a proton and an electron to an organic substrate in a concerted process, enables a single-electron reduction of compounds with very negative reduction potentials. In reactions that exploit PCET, an interaction between a carbonyl/iminyl group and an acid activator lowers the energy barrier during the SET process, and thus facilitates the formation of a ketyl/ $\alpha$ -aminoalkyl anion radical intermediates, which would otherwise be inaccessible *via* separate proton- and electron-transfer steps.<sup>53, 54, 69-71</sup>

### Scope of the review

Over the past decade, ketyl and  $\alpha$ -aminoalkyl anion radicals generated from aldehydes, ketones, and imines under photoredox conditions have been shown to undergo a diverse array of new C–C bond forming transformations, which provided convenient synthetic routes to medicinally relevant building blocks.<sup>72</sup> Most remarkably, the area of catalytic asymmetric radical coupling reactions has enjoyed tremendous growth, and thus a number of these ketyl/ $\alpha$ -amino radical reactions have been accomplished in an enantioselective

fashion. The purpose of this Review is to provide an overview of the important precedents that laid the foundation for photocatalytic coupling reactions of carbonyl and iminyl derivatives, and the recent (2008-2017) progress in the field. Radical-radical coupling reactions, radical additions to  $\pi$ -systems, as well as other reactions initiated by a single-electron reduction of carbonyl or iminyl moieties along with their proposed mechanisms, are discussed herein.

## Functionalization of $\alpha$ -C–X bond of ketones *via* ketyl radical intermediates

In late 1970s, Kellogg and coworkers published their seminal studies describing the reduction of phenacyl onium salts (sulfonium, ammonium, phosphonium) with *N*-substituted 1,4-dihydropyridines in the presence of  $\text{Ru}^{\text{II}}(\text{bpy})_2\text{Cl}_2$  (Scheme 2).<sup>44, 73</sup> While the reaction was very sluggish in the dark or in the absence of a photoredox catalyst, a significant rate enhancement was observed upon addition of a catalytic amount of  $\text{Ru}^{\text{II}}(\text{bpy})_3\text{Cl}_2$  to the reaction mixture. In addition to having higher rates, the reactions performed in the presence of  $\text{Ru}^{\text{II}}(\text{bpy})_3\text{Cl}_2$  were characterized by their cleanness and a lack of competing rearrangement of *N*-substituted 1,4-dihydropyridines.

Following the initial Kellogg's report, the ability of photoredox catalysts to reduce ketone-activated  $\alpha$ -C–X bonds, where X = Cl, Br, N, O, S, P, has been widely explored.<sup>61, 73-78</sup> Single-electron transfer to a  $\alpha$ -carbonyl compound generates an anion radical, which can be represented either as a carbon radical bonded directly to a negatively charged oxygen **3.2**, or its mesomeric structure containing a radical positioned on oxygen attached to a negatively charged carbon atom **3.3** (Scheme 3). This anion radical is known to undergo mesolysis – a fragmentation to afford an anion,  $\text{X}^-$ , and the  $\alpha$ -carbonyl radical **3.4**. The  $\alpha$ -carbonyl radical can then either abstract a hydrogen atom to yield a reduced product, or undergo a further transformation, such as a coupling reaction with another radical or an addition to a  $\pi$ -bond.

An interesting example of a photoredox reduction of  $\alpha$ -halocarbonyl reduction was reported in 1990 by Fukuzumi and co-workers.<sup>77</sup> Phenacyl halides (bromides and chlorides) were efficiently converted to acetophenones using  $\text{Ru}^{\text{II}}(\text{bpy})_3\text{Cl}_2$  as a photocatalyst and 10-methyl-9,10-dihydroacridine as the stoichiometric reductant (Scheme 4). The authors also observed that the addition of perchloric acid improved the product yields.

Based on the quenching experiments, the authors proposed that in the absence of acid, the reaction proceeds *via* reductive quenching of  $^*\text{Ru}^{\text{II}}(\text{bpy})_3^{2+}$  by  $\text{ArCH}_2$  (**5.4**) ( $E_{1/2}^{\text{red}} = +0.80$  V vs. SCE)<sup>79</sup> generating  $\text{Ru}^{\text{I}}(\text{bpy})_3^+$  reductant and cation radical  $\text{ArCH}_2^{\bullet+}$  (**5.5**) (Scheme 5). The Ru(I) species may then reduce phenacyl bromide (**5.1**) to form  $\alpha$ -carbonyl radical **5.2** and  $\text{Ru}^{\text{II}}(\text{bpy})_3^{2+}$  species. The  $\alpha$ -carbonyl radical can then abstract a hydrogen atom from cation radical  $\text{ArCH}_2^{\bullet+}$  (**5.5**) to generate the final product **5.3** and by-product  $\text{ArCH}^+$  (**5.6**). Conversely, in the presence of  $\text{HClO}_4$ ,  $^*\text{Ru}^{\text{II}}(\text{bpy})_3^{2+}$  reduces either protonated or acid-activated (*via* PCET) phenacyl halides producing strongly oxidizing  $\text{Ru}^{\text{III}}(\text{bpy})_3^{3+}$  *in situ*. Ru(III) can then oxidize  $\text{ArCH}_2$  (**5.4**) (or  $\text{ArCH}_3^+$  at a high concentration of the acid) to form  $\text{ArCH}_2^{\bullet+}$  (**5.5**) and regenerate Ru(II). The acetophenone product (**5.3**) is generated upon one-electron reduction of a ketyl radical **5.9** by  $\text{ArCH}^{\bullet}$  (**5.7**) followed by the loss of bromide and keto-enol tautomerization.

The ability of photoredox catalysts to reduce  $\alpha$ -heteroatom substituted ketones has also been utilized to achieve reductive opening of epoxides and aziridines (Scheme 6).<sup>61</sup> Due to the highly negative redox potentials of epoxides ( $E_{1/2}^{\text{red}} = -2.27$  V vs. Ag/AgI for stilbene oxide in DMF),<sup>80</sup> which precludes a direct electron transfer to the oxirane from Ru(I) or Ir(II), the authors installed an  $\alpha$ -carbonyl moiety as a relay. Positioning an epoxide or an aziridine next to the redox-active carbonyl group enabled their reductive opening with  $\text{Ru}^{\text{II}}(\text{bpy})_3^{2+}/\text{Ir}^{\text{III}}(\text{ppy})_2(\text{dtbppy})^+$  photocatalysts and Hantzsch ester (HEH) as a stoichiometric reductant. By performing the reaction in the presence of allyl sulfone, it was possible to obtain products of a reduction/allylation sequence.

Reductive opening of epoxides and aziridines **7.1** proceeds *via* a reductive quenching cycle of  $^*\text{Ru}^{\text{II}}(\text{bpy})_3^{2+}$  (Scheme 7). SET from HEH• (**7.7**) to  $^*\text{Ru}^{\text{II}}(\text{bpy})_3^{2+}$  forms a strong reductant,  $\text{Ru}^{\text{I}}(\text{bpy})_3^+$ . Reduction of epoxychalcone or  $\alpha$ -ketoaziridine **7.1** by  $\text{Ru}^{\text{I}}(\text{bpy})_3^+$  delivers a ketyl radical **7.2** and regenerates  $\text{Ru}^{\text{II}}(\text{bpy})_3^{2+}$  catalyst. Subsequently, ketyl radical **7.2** undergoes C–O or C–N bond cleavage to form anion radical **7.3**. Protonation by  $\text{PyH}^+$  (**7.8**) and a hydrogen atom abstraction from HEH (**7.6**) affords the  $\beta$ -hydroxy or  $\beta$ -aminoketone product **7.5**. Instead of undergoing hydrogen atom abstraction, the intermediate  $\alpha$ -carbonyl radical **7.3** can engage in allylation process with **7.10** to form a new C–C bond. This tandem ring-opening/allylation reaction affords  $\beta$ -hydroxy- $\alpha$ -allylketones **7.11** in good yields and high diastereoselectivity. It was found that the reduction of both epoxides and aziridines required an aryl substituent on the carbonyl group in order to enable the formation of a ketyl radical intermediate.

In 2016, Ma and Chen coupled a variety of carbonyl-group activated tertiary alkyl bromides with 4-alkyl Hantzsch esters and 4-alkyl Hantzsch nitriles under photocatalytic conditions to synthesize congested ketones, including ketones with all-carbon quaternary centers (Scheme 8).<sup>82</sup> In their approach, 4-substituted Hantzsch derivatives were used as alkyl radical precursors, which can release the  $\text{C}_{\text{sp}^3}$ -centered alkyl radicals upon a single electron oxidation.

It was proposed that the reaction starts with the photoexcitation of *fac*- $\text{Ir}^{\text{III}}(\text{ppy})_3$ . Oxidation of 4-alkyl Hantzsch ester (**9.4**) by  $^*\text{fac}\text{-Ir}^{\text{III}}(\text{ppy})_3$  in the presence of base generates radical **9.5** and Ir(II). Aromatization-driven C–C bond cleavage of radical **9.5**<sup>83</sup> gives benzylic radical **9.6** (Ar = Ph,  $E_{1/2}^{\text{red}} = -1.43$  V vs. SCE)<sup>84</sup> and a pyridine byproduct **9.8**. SET from the Ir(II) species ( $E_{1/2}^{\text{III/II}} = -2.19$  V vs SCE)<sup>85</sup> to  $\alpha$ -bromoketone **9.1** (R = Ph,  $E_{1/2}^{\text{red}} = -1.65$  V vs SCE)<sup>82</sup> regenerates Ir(III) and furnishes anion radical **9.2**, which subsequently undergoes mesolysis to  $\alpha$ -carbonyl radical **9.3** and bromide. Radical recombination between **9.3** and **9.6** affords the product **9.7**. An alternative pathway, in which anion radical **9.2** directly recombines with **9.6**, is also viable based on computational studies.

In 2017, Landais and co-workers utilized photoredox-catalysis to achieve intramolecular carboarylation of cyclopropenes with phenacyl bromides (Scheme 10).<sup>86</sup> Naphthalenones were obtained in moderate yields from both  $\alpha$ -bromoacetophenones and heteroaryl  $\alpha$ -bromoketones.

The reaction has been proposed to proceed *via* an oxidative quenching cycle of Ir(III) as depicted in Scheme 11. The  $\alpha$ -carbonyl radical **11.2** formed upon reduction of  $\alpha$ -bromoacetophenone (**11.1**) by the excited state photocatalyst,  $^*fac\text{-Ir}^{\text{III}}(\text{ppy})_3$  ( $E_{1/2}^{\text{IV}/^*\text{III}} = -1.73$  V vs SCE),<sup>85, 87</sup> undergoes addition to cyclopropene **11.3** to generate cyclopropyl radical **11.4**. Intramolecular addition of **11.4** to the arene moiety provides cyclohexadienyl radical **11.5**, which is then oxidized by Ir(IV) species to **11.6**, and deprotonated under basic conditions to afford cyclopropane **11.7**. Naphthalenone **11.8** is then obtained upon deprotonation of **11.7**  $\alpha$  to the ketone followed by the opening of the cyclopropane ring and protonation.

## Radical-radical coupling reactions

The earliest literature example which invokes the formation of a ketyl radical and its subsequent recombination with another radical species under photoredox conditions was reported by Pac in 1983.<sup>88</sup> Pac and co-workers described their studies on the reduction of (hetero)aromatic aldehydes and ketones under visible light irradiation with *N*-benzyl-1,4-dihydronicotinamide (BNAH) as a stoichiometric reductant and  $\text{Ru}^{\text{II}}(\text{bpy})_3\text{Cl}_2$  as a photon-absorbing catalyst (Scheme 12). The authors found that the course of the reaction was strongly dependent on the structural and electronic parameters of the carbonyl compounds used. While benzaldehydes and trifluoroacetophenone were preferentially converted to coupling adducts **12.2**, di-2-pyridylketone was almost quantitatively reduced to the corresponding alcohol **12.1** without formation of any adduct. The authors argued that the exclusive reduction of di-2-pyridylketone to di-2-pyridinylmethanol can be attributed to the two pyridyl groups attached to the carbonyl group. The pyridyl substituents are strongly electron-withdrawing and thus facilitate the one-electron reduction of the intermediate radical  $\text{HO-C}\cdot(2\text{-py})_2$ . In addition, the steric hindrance of radical  $\text{HO-C}\cdot(2\text{-py})_2$ , bearing two large pyridyl groups, inhibits the radical coupling reaction and prevents the formation of the adduct **12.2**.

It was proposed that the reaction proceeds as outlined in Scheme 13.<sup>88, 89</sup> Reduction of excited  $^*\text{Ru}^{\text{II}}(\text{bpy})_3^{2+}$  ( $E_{1/2}^{^*\text{III}/\text{I}} = +0.77$  V vs SCE)<sup>66</sup> by BNAH (**13.3**) ( $E_{1/2}^{\text{red}} = +0.639$  V vs SCE)<sup>83</sup> gives  $\text{Ru}^{\text{I}}(\text{bpy})_3^+$  and  $\text{BNAH}\cdot^+$  (**13.4**).  $\text{Ru}^{\text{I}}(\text{bpy})_3^+$  ( $E_{1/2}^{\text{red}} = -1.33$  V vs SCE)<sup>66</sup> reduces the carbonyl compound **13.1** presumably *via* PCET to a ketyl radical **13.2**. The ketyl radical **13.2** can then recombine with  $\text{BNA}\cdot$  (**13.5**) (formed upon deprotonation of  $\text{BNAH}\cdot^+$ ) to afford **13.8** or undergo a competitive one-electron reduction by  $\text{BNA}\cdot$  (**13.5**) or BNAH (**13.3**) to generate **13.7**. Recombination of two  $\text{BNA}\cdot$  radicals (**13.5**) leads to the formation of a side product **13.9**.

Following initial studies by Pac et al. on photoredox-catalysed reactions of aromatic aldehydes and ketones with BNAH, ketyl and  $\alpha$ -aminoalkyl anion radicals generated from carbonyl derivatives upon a single-electron reduction have been employed in a number of radical homo- and heterocoupling reactions. For instance, in 2013, MacMillan and co-workers developed a strategy for direct  $\beta$ -functionalization of cyclic ketones with aryl ketones (Scheme 14) by merging photoredox and organocatalysis.<sup>52</sup> The products are formed in good yields and moderate to good diastereoselectivities upon coupling of benzophenone with cyclohexanones bearing both alkyl and aryl substituents at the 3-, and 4-

positions (Scheme 14). The reaction also works well with cyclopentanone (65% yield); however, lower yields (10-20%) of the desired  $\beta$ -alkyloxy products are observed when 7-membered ketones are employed as substrates. In terms of ketyl radical precursors, the reaction tolerates a range of substituted benzophenones. Aryl-alkyl ketones, however, being more difficult to reduce than biaryl ketones ( $E_{1/2}^{\text{red}} = -2.11$  V vs SCE for acetophenone),<sup>5</sup> do not undergo the desired coupling reaction when  $\text{Ir}^{\text{III}}(\text{ppy})_3$  is employed as the photocatalyst. Expansion of the scope of ketyl-radical partners and coupling of both electron-rich and electron-poor acetophenone derivatives have been facilitated by the use of  $\text{Ir}^{\text{III}}(p\text{-OMe-ppy})_3$ .

MacMillan et. al. proposed that the photocatalytic synthesis of  $\gamma$ -hydroxyketones proceeds as illustrated in Scheme 15. Irradiation of  $\text{Ir}^{\text{III}}(\text{ppy})_3$  with visible light produces  $^*\text{Ir}^{\text{III}}(\text{ppy})_3$ , which is sufficiently reducing ( $E_{1/2}^{\text{IV}/^*\text{III}} = -1.73$  V vs SCE)<sup>85, 87</sup> to engage in a SET process in the presence of acetic acid – the reduction potential of benzophenone ( $E_{1/2}^{\text{red}} = -1.83$  V vs SCE)<sup>91</sup> is elevated in acidic medium through hydrogen bonding interactions, which renders the C=O bond reduction thermodynamically feasible. An electron transfer from  $^*\text{Ir}^{\text{III}}(\text{ppy})_3$  to the aryl ketone **15.1** affords a strongly oxidizing  $\text{Ir}^{\text{IV}}(\text{ppy})_3^+$  and the corresponding ketyl radical **15.2**.  $\text{Ir}^{\text{IV}}(\text{ppy})_3^+$  ( $E_{1/2}^{\text{IV}/\text{III}} = +0.77$  V vs SCE)<sup>85</sup> then oxidizes an electron-rich enamine **15.5** ( $E_{1/2}^{\text{red}} = +0.385$  V vs SCE for **15.5**)<sup>92</sup> formed upon condensation of amine catalyst **15.4** with the ketone coupling partner **15.3**. A subsequent proton loss from the oxidized enamine **15.6** generates an enaminy radical **15.7**, which readily recombines with the ketyl radical **15.2** to generate  $\gamma$ -hydroxyketone enamine **15.8**. Enamine hydrolysis affords the desired  $\gamma$ -hydroxyketone product **15.9**, regenerates the secondary amine catalyst **15.4** and completes the organocatalytic cycle. With  $\text{Ir}^{\text{III}}(p\text{-OMe-ppy})_3$  the reaction proceeds *via* an alternative pathway, in which oxidation of the enamine precedes the reduction of acetophenone, as evidenced by Stern-Volmer quenching experiments: while the emission of  $^*\text{Ir}^{\text{III}}(\text{ppy})_3$  is readily quenched by benzophenone, neither acetophenone or acetophenone in the presence of acetic acid can quench the excited state of  $\text{Ir}^{\text{III}}(p\text{-OMe-ppy})_3$ . In contrast, emission of  $^*\text{Ir}^{\text{III}}(p\text{-OMe-ppy})_3$  is efficiently quenched by the enamine generated from cyclohexanone and azepane.

In 2015, MacMillan et. al. reported that in analogy to  $\gamma$ -hydroxyketones, racemic  $\gamma$ -aminoketones can be synthesized *via* coupling of  $\beta$ -enaminy radicals with  $\alpha$ -amino radicals under photoredox conditions with  $\text{Ir}^{\text{III}}(\text{ppy})_2(\text{dtbbpy})\text{PF}_6$  catalyst.<sup>63</sup> The reaction is applicable to a wide range of imine coupling partners: aldimines, diaryl and aryl-alkyl ketimines furnish the desired  $\gamma$ -aminoketones in high yields (Scheme 16). With regard to the  $\beta$ -enaminy radical precursors, cyclohexanone derivatives with substituents at 2-, 3-, and 4-positions as well as cyclopentanones readily undergo the  $\beta$ -aminoalkyl ketone-forming reaction.

The reaction is suggested to proceed *via* reductive quenching of  $^*\text{Ir}^{\text{III}}(\text{ppy})_2(\text{dtbbpy})^+$  ( $E_{1/2}^{\text{III}/\text{II}} = +0.66$  V vs SCE)<sup>93</sup> by DABCO (**17.3**) ( $E_{1/2}^{\text{red}} = +0.69$  V vs SCE)<sup>94</sup> (Scheme 17). In this process, DABCO cation radical (DABCO<sup>+</sup>) (**17.4**) and the strongly reducing  $\text{Ir}^{\text{II}}(\text{ppy})_2(\text{dtbbpy})$  ( $E_{1/2}^{\text{III}/\text{II}} = -1.51$  V vs SCE)<sup>93</sup> are generated. Subsequent reduction of **17.4** by the electron-rich enamine **17.7** ( $E_{1/2}^{\text{red}} = +0.385$  V vs SCE for **17.7**)<sup>92</sup> affords enaminylation radical **17.8** and regenerates DABCO, which acts as an electron transfer



agent. A SET from Ir<sup>II</sup>(ppy)<sub>2</sub>(dtbbpy) to a protonated imine **17.1** forges  $\alpha$ -amino radical **17.2**, which undergoes radical-radical coupling with  $\beta$ -enaminy radical **17.9**, formed upon deprotonation of **17.8**. Hydrolysis of the resulting  $\gamma$ -aminoketone enamine **17.10** furnishes the final  $\gamma$ -aminoketone product **17.11**. The proposed mechanism is corroborated by (i) Stern-Volmer quenching studies, according to which DABCO is a better quencher of the excited photocatalyst than enamine; and (ii) significant drop in the reaction efficiency upon lowering the loading of DABCO.

In 2014, MacMillan and coworkers demonstrated that  $\alpha$ -amino radicals generated from imines can efficiently couple with benzylic ether radicals to furnish a variety of  $\beta$ -amino ether products.<sup>95</sup> Various oxygen-protecting groups, cyclic ethers, and heteroaromatic-containing ethers are well tolerated under the optimized conditions. With regard to the aldimine substrate, high yields can be obtained with electron-rich, electron-poor, as well as heteroaromatic substituents on both the aldehyde- and imine-derived moieties of the imine (Scheme 18).

It was proposed that the key to achieve the desired reactivity is the combination of an iridium photocatalyst with a thiol organocatalyst (Scheme 20). Upon irradiation with blue light, Ir<sup>III</sup>(ppy)<sub>2</sub>(dtbbpy)<sup>+</sup> undergoes photoexcitation to give a long-lived ( $\tau = 557$  ns)<sup>96</sup> excited state, \*Ir<sup>III</sup>(ppy)<sub>2</sub>(dtbbpy)<sup>+</sup>. This \*Ir<sup>III</sup> species can act as an oxidant ( $E_{1/2}^{*III/II} = +0.66$  V vs SCE)<sup>93</sup> and accept an electron from the thiol organocatalyst methyl thioglycolate (**20.3**) to form Ir<sup>II</sup>(ppy)<sub>2</sub>(dtbbpy) and thiyl radical **20.4**. The authors argued that this electron transfer step is facilitated by the weakly basic additive, LiOAc, and proceeds *via* a concerted PCET event. Abstraction of a hydrogen atom (HAT) from benzyl ether **20.5** affords benzylic ether radical **20.6** and regenerates the thiol catalyst. A C–C bond forming coupling reaction between a benzylic ether radical **20.6** and an  $\alpha$ -aminoanion radical **20.2**, generated upon a single electron reduction of imine **20.1** ( $E_{1/2}^{red} = -1.91$  V vs SCE for *N*-benzylideneaniline)<sup>5</sup> by Ir<sup>II</sup>(ppy)<sub>2</sub>(dtbbpy) ( $E_{1/2}^{III/II} = -1.51$  V vs SCE)<sup>93</sup>, yields the final  $\beta$ -amino ether product **20.7**.

Ketyl and  $\alpha$ -aminoalkyl anion radicals are known to undergo C–C bond-forming homocoupling reactions to furnish pinacol and imino-pinacol products, respectively. In 2015, Rueping and co-workers reported that such a transformation can proceed efficiently under visible light photoredox conditions (Scheme 21 and Scheme 22).<sup>56</sup> In case of the pinacol coupling of aldehydes and ketones, the protocol is applicable to the synthesis of diols derived from benzaldehydes bearing electron-donating and electron-withdrawing groups, as well as both electron-poor aromatic and aliphatic ketones. In this transformation, Ir<sup>III</sup>[F(CF<sub>3</sub>)ppy]<sub>2</sub>(bpy)PF<sub>6</sub> is employed as a photoredox catalyst, while tributylamine plays a dual role – it not only acts as an electron donor, but also serves as a precursor to a radical cation, which activates the carbonyl substrates in the reduction step.

Under slightly modified reaction conditions, imines were found to undergo photoredox-catalysed imino-pinacol coupling reaction to yield symmetric diamines in good yields (Scheme 22).

The postulated mechanism for the photoredox-catalysed reductive coupling of carbonyl derivatives developed by Rueping et al. is depicted in Scheme 23. The reaction is initiated by visible light-induced photoexcitation of  $\text{Ir}^{\text{III}}[\text{F}(\text{CF}_3)\text{ppy}]_2(\text{bpy})^+$  to its excited state,  $^*\text{Ir}^{\text{III}}[\text{F}(\text{CF}_3)\text{ppy}]_2(\text{bpy})^+$ . Reductive quenching of  $^*\text{Ir}^{\text{III}}[\text{F}(\text{CF}_3)\text{ppy}]_2(\text{bpy})^+$  by  $\text{NBu}_3$  affords  $\text{Ir}^{\text{II}}[\text{F}(\text{CF}_3)\text{ppy}]_2(\text{bpy})$  ( $E_{1/2}^{\text{III/II}} = -1.31 \text{ V vs SCE}$ )<sup>56</sup> and cation radical **23.2**. The resulting Lewis acidic cation radical **23.2** can interact with the weakly basic C=O (or C=N) bond of a carbonyl compound through a two-center/three-electron bond. This interaction facilitates the reduction of species **23.4** by  $\text{Ir}^{\text{II}}[\text{F}(\text{CF}_3)\text{ppy}]_2(\text{bpy})$  to a ketyl radical by lowering the energy barrier for the SET process. Alternatively, the carbonyl group can be activated by the  $\alpha$ -ammonium radical **23.3** generated from **23.2** via a [1,2]-H shift. The so-formed **23.5** can then engage in hydrogen-bonding interaction with a C=O bond and thus enable ketyl radical **23.6** formation. Homocoupling of two **23.6** followed by protonation affords the desired product **23.7**.

In 2015, Ooi et al.<sup>64</sup> utilized an elegant dual catalytic system comprising a photoredox catalyst and a chiral Brønsted acid to achieve an asymmetric  $\alpha$ -coupling of *N*-sulfonyl imines with *N*-arylaminoethanes (Scheme 24). Unsymmetrical chiral vicinal diamines were obtained in high yields and excellent enantioselectivities (up to 97% ee) from a wide range of aryl and heteroaryl *N*-sulfonyl aldimines. With respect to the aminomethyl radical precursor, both *N,N*-diarylaminoethanes and *N*-alkyl-*N*-arylaminoethanes were suitable reaction partners for the  $\alpha$ -coupling process. Development of the catalytic enantioselective coupling protocol by Ooi has been a remarkable milestone in the field of asymmetric radical chemistry as the precise control of the high intrinsic reactivity of odd-electron species is considered a formidable challenge in organic synthesis.

The reaction has been proposed to proceed via a reductive quenching pathway of the iridium photocatalyst as depicted in Scheme 25. The process is initiated by irradiation of  $\text{Ir}^{\text{III}}(\text{ppy})_2(\text{Me}_2\text{phen})^+$  with visible light, followed by a single electron reduction of  $^*\text{Ir}^{\text{III}}(\text{ppy})_2(\text{Me}_2\text{phen})^+$  by  $\text{Ph}_2\text{NMe}$  (**25.1**). A SET from  $\text{Ir}^{\text{II}}(\text{ppy})_2(\text{Me}_2\text{phen})$  ( $E_{1/2}^{\text{III/II}} = -1.58 \text{ V vs SCE}$ )<sup>64</sup> to *N*-sulfonyl imine **25.4** ( $E_{1/2}^{\text{red}} = -1.45 \text{ V vs SCE}$  for *N*-benzylidenemethanesulfonamide)<sup>64</sup> produces  $\alpha$ -aminoanion radical **25.5** and regenerates the active photocatalyst. Catalytic ion pair formation between *P*-spiro chiral tetraaminophosphonium cation **25.6** and **25.5** enables an enantioselective radical coupling reaction between **25.5** and aminomethyl radical **25.3** to afford the desired diamine product **25.7**.

A conceptually similar reaction was reported by Rueping et al. in 2016.<sup>58</sup> In this case, the coupling between aldimines and tertiary amines yielding unsymmetrical vicinal diamines was accomplished with the use of  $\text{Ir}^{\text{III}}(\text{ppy})_2(\text{dtbbpy})\text{PF}_6$  as a photoredox catalyst (Scheme 26). With respect to the amine-derived part of the imine moiety, the reaction tolerated both electron-rich and electron-poor (hetero)aromatic substrates with different substitution patterns. In terms of the aldehyde-derived R<sup>1</sup>-substituent, imines containing aryl, heteroaryl, and carbonyl group underwent coupling reaction in good yields. Under Rueping's conditions, a range of *N,N*-disubstituted aniline derivatives were converted into the desired diamine products in moderate to good yields. In addition, coupling of a two secondary  $\alpha$ -



amino radical fragments was enabled by an introduction of an electrofugal groups (TMS or CO<sub>2</sub>H) onto the methylene moiety of the amine partner.

Rueping et. al. also demonstrated that their reductive coupling protocol is applicable to the synthesis of vicinal aminoalcohols *via* recombination of ketyl and  $\alpha$ -amino radicals (Scheme 27). Differently-substituted benzaldehydes as well as pyridinecarboxaldehyde successfully provided the desired products. The authors also noted that addition of catalytic amounts of benzoic acid had a beneficial influence on the reactions: it enabled the coupling to proceed faster and with lower catalyst loading (0.5 mol%).

A proposed mechanism for the Rueping's synthesis of 1,2-aminoalcohols is illustrated in Scheme 28. Reductive quenching of \*Ir<sup>III</sup>(ppy)<sub>2</sub>(dtbbpy)<sup>+</sup> by amine **28.1**, followed by a single-electron reduction of aldehyde **28.4** by Ir<sup>II</sup>(ppy)<sub>2</sub>(dtbbpy) generates the ketyl radical **28.5**, which couples with the  $\alpha$ -amino radical **28.3** to provide the final product **28.7** upon protonation of **28.6**.

In 2016, Meggers and co-workers employed a chiral metal photocatalyst ( $\wedge$ -**IrS**) to develop a novel catalytic enantio- and diastereoselective synthesis of 1,2-amino alcohols from trifluoromethyl ketones and tertiary amines (Scheme 29).<sup>62</sup> A variety of aromatic amines can be used in this transformation to afford the desired coupling products in high yields and excellent enantioselectivities (up to 99% ee). The scope of this reaction, however, is limited to heteroaryl trifluoromethyl ketones that are sufficiently electron-deficient to undergo a single-electron reduction process and possess two coordinating directing groups through which they can bind to the chiral metal center.

The authors postulated that the mechanism involves a SET from a tertiary amine **30.4** to the photoexcited \*Ir(III)-bound ketone **30.3**, which generates an amino cation radical **30.6** and an iridium-coordinated ketyl radical **30.5** (Scheme 30).<sup>62</sup> Subsequent proton transfer and radical-radical cross-coupling between **30.7** and **30.8** affords the Ir(III)-bound 1,2-amino alcohol product **30.9**, which is then replaced by new substrate **30.1**. In this transformation, the chiral iridium complex acts both as a photoredox catalyst, and a Lewis acid that activates ketones for the reduction process and controls the stereochemistry of the radical-radical cross-coupling step.

In their subsequent work, Meggers et al. extended the scope of the coupling reaction from ketones containing the  $\alpha$ -CF<sub>3</sub> group to a range of 2-acyl imidazoles (Scheme 31).<sup>97</sup> The chiral-at-the metal rhodium-based Lewis acid  $\wedge$ -**RhS** was employed in combination with Ru(bpy)<sub>3</sub>(PF<sub>6</sub>)<sub>2</sub> photoredox catalyst to facilitate the reaction between ketones and  $\alpha$ -silylamines. Chiral 1,2-aminoalcohols were obtained in high yields and excellent enantioselectivities from both aromatic and aliphatic 2-acyl imidazoles and differently substituted  $\alpha$ -trimethylsilylalkylamines.

The process begins with absorption of visible light by Ru<sup>II</sup>(bpy)<sub>3</sub><sup>2+</sup> to give photoexcited \*Ru<sup>II</sup>(bpy)<sub>3</sub><sup>2+</sup>. \*Ru<sup>II</sup>(bpy)<sub>3</sub><sup>2+</sup> ( $E_{1/2}^{*II/I} = +0.77$  V vs SCE)<sup>66</sup> is sufficiently oxidizing to accept an electron from  $\alpha$ -silylamine **32.1** ( $E_{1/2}^{\text{red}} = +0.41$  V vs SCE for *N*-phenyl-*N*-((trimethylsilyl)methyl)aniline),<sup>98</sup> generating Ru<sup>I</sup>(bpy)<sub>3</sub><sup>+</sup> species and a cation radical **32.2**,

which undergoes rapid silyl transfer with Rh-bound ketone **32.5** to afford an  $\alpha$ -aminomethyl radical **32.3** and an electron deficient silylated intermediate **32.6**. A SET from  $\text{Ru}^{\text{I}}(\text{bpy})_3^+$  ( $E_{1/2}^{\text{II/I}} = -1.33$  V vs SCE)<sup>66</sup> to **32.6** forms a rhodium coordinated, silylated ketyl radical **32.7**, which subsequently undergoes a radical-radical coupling reaction with the  $\alpha$ -aminomethyl radical **32.3** to afford Rh-bound coupled product **32.8**. Release of the 1,2-aminoalcohol **32.9** and coordination of a new substrate **32.4** completes the catalytic cycle.

In 2017, Xia group reported that ketyl and  $\alpha$ -aminoalkyl radicals can undergo intermolecular coupling reaction with anion radicals derived from dicyanobenzenes or isonicotinonitrile to afford arylation products (Scheme 33).<sup>99</sup> This photocatalytic protocol is applicable to a broad range of aromatic aldehydes, ketones, and imines, and allows access to secondary/tertiary alcohols and amines under mild reaction conditions in moderate to excellent yields.

In analogy to the Rueping's protocol,<sup>56</sup> it has been proposed that the C=X bond reduction is enabled by the interaction with the  $\alpha$ -ammonium radical **34.3** (or the Lewis acidic cation radical **34.2**) (Scheme 34). PCET from  $\text{Ir}^{\text{II}}(\text{ppy})_2(\text{dtbbpy})$  ( $E_{1/2}^{\text{III/II}} = -1.51$  V vs SCE)<sup>93</sup> to **34.4** (or, alternatively, to **34.5**) leads to the formation of ketyl or  $\alpha$ -aminoalkyl radical **34.6**, which undergoes intermolecular radical-radical cross-coupling with **34.8**, formed in the second photoredox cycle upon a single electron reduction of **34.7** by  $\text{Ir}^{\text{II}}(\text{ppy})_2(\text{dtbbpy})$ . Subsequent elimination of the cyanide anion from **34.9** affords the desired product **34.10**.

## Reactions of enones and cyclopropylketones via ketyl radical intermediates

The reactivity of conjugated ketyl radical intermediates generated from enones in the presence of Lewis/Brønsted acid activators was extensively studied by the Yoon group. Enones, whose reduction potential is elevated by coordination to an acid, have been reported to engage in a number of photocatalytic cycloaddition reactions. For example, in 2008, Yoon demonstrated that (hetero)aryl enones readily react with pendant Michael acceptors in the presence of the Lewis acid to yield *cis* products of intramolecular [2+2] cycloaddition (Scheme 35).<sup>47</sup> Aliphatic enones and enoates, which are more difficult to reduce, do not form the desired products under the reaction conditions. Subsequently, Yoon developed intermolecular versions of this reaction, which enabled an access to crossed [2+2] heterodimers.<sup>48, 100</sup> Aryl enones were efficiently coupled with suitable  $\alpha,\beta$ -unsaturated carbonyl derivatives to yield *trans* cycloaddition products (Scheme 36). The competing homodimerization was successfully suppressed provided that aryl enones were both (i) more readily reducible, and (ii) less reactive than their corresponding Michael acceptor coupling partners.

Yoon proposed that the cycloaddition reaction proceeds *via* a reductive quenching cycle of  $^*\text{Ru}^{\text{II}}(\text{bpy})_3^{2+}$  as depicted in Scheme 37.  $\text{Ru}^{\text{I}}(\text{bpy})_3^+$ , formed upon reduction of  $^*\text{Ru}^{\text{II}}(\text{bpy})_3^{2+}$  by Hünig's base, transfers an electron to the lithium-activated enone **37.2** to furnish an enone anion radical **37.3**, initiating the [2+2] cycloaddition process with **37.4** and regenerating the  $\text{Ru}^{\text{II}}(\text{bpy})_3^{2+}$  photocatalyst. Since aryl enones are significantly easier to be reduced than less-conjugated enone substrates,<sup>101</sup> the coupling reaction can be performed with high chemoselectivity.

In 2014, Yoon reported an asymmetric variant of the intermolecular [2+2] enone cycloaddition (Scheme 38).<sup>55</sup> Since no background reaction takes place in the absence of a Lewis acid due to the need for enone activation towards a single-electron reduction, high enantioselectivities of 1,2-*trans* cyclobutane products could be obtained by using a combination of a Lewis acid, Eu(OTf)<sub>3</sub>, and a chiral ligand **38.1**. The cyclization reaction proceeded in good yields for enones bearing both electron-rich and electron poor aryl rings, heteroaryl enones, as well as  $\gamma$ -substituted enones.

While bis(enones) with a three-carbon tether were shown to undergo [2+2] cycloaddition, <sup>47, 100</sup> reaction of bis(enones) with a longer aliphatic tether length under similar photoreductive conditions led to the formation of [4+2] hetero Diels-Alder cycloadducts (Scheme 39).<sup>50</sup> Notably, Yoon's photoredox conditions facilitated coupling between an electron-deficient diene and an electron-poor dienophile, which is normally difficult to achieve upon thermal activation. In this process, Mg(ClO<sub>4</sub>)<sub>2</sub> was found to be the optimal Lewis acid, which enabled the right balance between substrate activation for the SET step and an undesired reductive decomposition of the cycloaddition product. Symmetrical aryl enones bearing electron-rich and electron-poor substituents and heteroaryl enones were well tolerated under the optimized conditions. The reaction was also found to be applicable to unsymmetrical aryl-alkyl enones, although slightly diminished yields were observed with these substrates.

The photocatalytic [4+2] hetero Diels-Alder cycloaddition reaction has been proposed to proceed as depicted in Scheme 40. Reduction of \*Ru<sup>II</sup>(bpy)<sub>3</sub><sup>2+</sup> by Hünig's base generates Ru<sup>I</sup>(bpy)<sub>3</sub><sup>+</sup>, a reductant which engages in a SET with the Lewis-acid activated aryl enone **40.2** (the rate of a one-electron reduction of methyl enone was found to be much slower than the rate of the reduction of aryl enone). Intramolecular cyclization of anion radical **40.3** affords *trans*-substituted cyclohexane intermediate **40.4**, which isomerizes to the more stable aryl ketyl radical **40.5**. The key step is the selective formation of the C–O bond from **40.5**. Subsequently, loss of an electron either to the photogenerated amine cation radical or another equivalent of enone affords the [4+2] hetero Diels-Alder cycloaddition product **40.7**.

Yoon et al. also reported that aryl cyclopropyl ketones react with olefins to afford highly substituted cyclopentane rings under similar photoredox conditions (Scheme 41).<sup>102</sup> In contrast to the [2+2] cycloaddition reaction, this [3+2] process was found to be applicable to substrates containing not only pendant enone acceptors, but also styrenes, cyclic aliphatic olefins, as well as aryl and aliphatic alkynes. In addition, it was empirically determined that LiBF<sub>4</sub> was not sufficiently Lewis acidic to activate cyclopropyl ketones towards the single-electron reduction; a more strongly acidic Lewis acid additive, La(OTf)<sub>3</sub>, was required to facilitate the reaction.

More recently, the Yoon group reported an asymmetric intermolecular version of the [3+2] cycloaddition process (Scheme 42).<sup>57</sup> The enantioselectivity of the reaction was controlled by the use of a catalytic amount of Gd(III) pybox complex. It was demonstrated that a wide range of aryl and heteroaryl cyclopropyl ketones could undergo the coupling reaction with styrenes, *N*-vinylcarbazole, and conjugated dienes to afford densely substituted

cyclopentanes in excellent yields with high enantioselectivities and moderate diastereoselectivities.

Scheme 43 depicts the working hypothesis of the mechanism of the [3+2] cycloaddition process. In analogy to the previously discussed examples, this transformation is proposed to proceed *via* reductive quenching cycle of  $*\text{Ru}^{\text{II}}(\text{bpy})_3^{2+}$ .  $\text{Ru}^{\text{I}}(\text{bpy})_3^+$  transfers an electron to phenyl ketone activated by the chiral Gd(III) Lewis acid complex **43.1**. The SET yields a ketyl radical **43.2**, which undergoes a cyclopropyl ring opening followed by alkene addition, cyclization and reoxidation. The formation of a neutral product **43.7** can occur either by chain-terminating reduction of the photogenerated amine cation radical or by chain-propagating electron-transfer to another equivalent of Gd(III)-activated substrate **43.1**.

Interestingly, Yoon et. al. observed that the outcome of the photocatalytic reaction of enones strongly depends on the nature of the acid co-catalyst employed for the substrate activation.<sup>47, 49</sup> While Lewis acids, for instance  $\text{LiBF}_4$ , promote the [2+2] cycloaddition, Brønsted acids, such as  $\text{HCO}_2\text{H}$ , have been reported to favor the reductive coupling reaction (Scheme 44). Notably, these two reactions differ by their overall redox balance: the [2+2] cycloaddition is net redox-neutral, whereas the reductive cyclization constitutes a two-electron reduction of the enone substrate. It was argued that the reactivity of the neutral radical intermediate formed in the presence of a Brønsted acid is very distinct from the chemistry of the anion radical generated under Lewis acidic conditions: the neutral radical preferentially undergoes 5-*exo*-trig cyclization rather than the [2+2] cycloaddition. Thus, the acid co-catalyst determines the nature of the reactive intermediate, which, in turn, has a profound influence on the overall transformation, its stereoselectivity, and oxidation state of the products.

It is worth noting that the photoreductive cyclization of enones, in contrast to the [2+2] cycloaddition reaction, is applicable to aliphatic enones, activated alkynes and styrenes, and is generally *trans* selective (Scheme 45).<sup>49</sup>

Another net reductive coupling reaction under photoredox conditions involving conjugated ketyl radical intermediates was reported by Xia and co-workers (Scheme 46).<sup>103</sup> Chalcones were shown to undergo reductive dimerization when treated with  $\text{Ru}^{\text{II}}(\text{bpy})_3(\text{PF}_6)_2$  photoredox catalyst,  $\text{Sm}(\text{OTf})_3$  Lewis acid and Hünig's base as the terminal reductant. Sm(III)-stabilized anion radical **46.2** was proposed to dimerize to generate dienolate **46.3**. Sequential protonation and intramolecular aldol reaction provided an access to polysubstituted cyclopentanol derivatives **46.5**. Nine examples were reported, and the reaction was shown to tolerate neither substitution at  $\beta$  and  $\beta$ -position nor *ortho*-substituted  $\text{Ar}^1$  groups.

In 2017, Gong and Meggers demonstrated that conjugated ketyl radicals undergo intermolecular enantioselective radical-radical coupling reaction with *N*-centered radicals derived from *N*-aryl carbamates (Scheme 47).<sup>104</sup> The conjugate amination of  $\alpha,\beta$ -unsaturated 2-acyl imidazoles proceeds with very high yields and excellent enantioselectivities in the presence of a chiral-at-rhodium Lewis acid catalyst  $-\text{RhO}$ , a weak phosphate base, and an iridium-based photoredox catalyst  $\text{Ir}^{\text{III}}[\text{dF}(\text{CF}_3)\text{ppy}]_2(5,5'\text{-dCF}_3\text{bpy})\text{PF}_6$ .

It was proposed that the reaction proceeds as depicted in Scheme 48.<sup>104</sup> A PCET to the photoexcited  $^*\text{Ir(III)}$  catalyst from the Brønsted-base-activated carbamate **48.1** generates a *N*-centered radical **48.2** and Ir(II) species. A single-electron reduction of the rhodium-coordinated substrate **48.3** by Ir(II) leads to the formation of rhodium enolate radical intermediate **48.4**, which subsequently undergoes recombines with the carbamoyl *N*-radical **48.2** to afford **48.5**. Protonation of **48.5** followed by product release from Scheme **48.6** and coordination of a new substrate to the chiral rhodium catalyst closes the catalytic cycle. The asymmetric induction providing *S*-configured products is governed by the *S*-configured rhodium catalyst.

Gong and Meggers also reported that under slightly modified reaction conditions 2-acyl imidazoles react with *N*-alkyl amides to furnish  $\delta$ -alkylation products (Scheme 49).<sup>105</sup> This asymmetric remote C(sp<sup>3</sup>)-H functionalization tolerated different  $\beta$ - and *N*-substituents on 2-acyl imidazole substrates; with regard to the amide coupling partner, the reaction was shown to work best with PMP-containing substrates, presumably due to the more facile oxidation of electron-rich amides under PCET conditions.

The alkylation reaction was proposed to proceed as depicted in Scheme 50 and follow the mechanism previously discussed for the  $\beta$ -amination of enones (Scheme 48).<sup>104, 105</sup> The amidyl radical **50.2** generated from **50.1** under PCET conditions was proposed to undergo an intramolecular 1,5-hydrogen atom transfer (1,5-HAT) to form a carbon-centered radical **50.3**. Radical-radical coupling between **50.3** and **50.5** furnishes the C-C bond in an enantioselective fashion.

## Addition of ketyl and $\alpha$ -aminyl anion radicals to $\pi$ -systems

Another important class of transformations characteristic of ketyl and  $\alpha$ -aminyl anion radicals are their additions to activated  $\pi$ -bonds. In 2013, Knowles and co-workers developed a new photocatalytic protocol for an intramolecular ketyl-olefin coupling reaction (Scheme 51) using the concept of proton-coupled electron transfer (PCET).<sup>54</sup> The cyclization was applicable to aryl ketones with pendant acrylate esters, acrylonitrile, and styrenyl acceptors.

Knowles et al. postulated that the reaction proceeds as depicted in Scheme 52. Photoexcitation of  $\text{Ru}^{\text{II}}(\text{bpy})_3^{2+}$  generates  $^*\text{Ru}^{\text{II}}(\text{bpy})_3^{2+}$ , which is proposed to be reduced to  $\text{Ru}^{\text{I}}(\text{bpy})_3^+$  by HEH. At the same time, the Brønsted acid catalyst can engage in reversible hydrogen-bonding interactions with the ketone substrate **52.1** to form a hydrogen-bonded Brønsted acid-ketone complex, which can participate in a concerted PCET. In this step, an electron transfer from the strongly reducing  $\text{Ru}^{\text{I}}(\text{bpy})_3^+$  occurs concomitantly with the proton transfer to the ketone oxygen to afford a neutral ketyl intermediate **52.2**. The ketyl radical **52.2** can then undergo an intramolecular Michael addition to form a cyclopentane ring and an  $\alpha$ -carbonyl radical **52.3**. Hydrogen atom abstraction from HEH by the  $\alpha$ -carbonyl radical **52.3** generates the final product **52.4** and HEH $\cdot$ . HEH $\cdot$ , being a strong reductant, can reduce  $^*\text{Ru}^{\text{II}}(\text{bpy})_3^{2+}$  and close the catalytic cycle upon proton transfer.

Also in 2013, Knowles group applied the concept of PCET into development of a highly enantioselective intramolecular azapinacol coupling reaction (Scheme 53).<sup>53</sup> The enantioselectivity of the reductive coupling of ketones and hydrazones was realized by the use of a chiral triphenylsilyl-substituted phosphoric acid. The coupling reaction proceeded with good yields and high enantioselectivities from both electron-rich and electron-poor acetophenone derivatives. Heterocyclic ketones were also tolerated, although an erosion in both yield and *ee* was observed in these cases.

In analogy to their previous work,<sup>53, 54</sup> the authors proposed that the reaction is initiated by an off-cycle excitation of the Ir(III) photocatalyst, followed by reduction of \*Ir(III) by HEH (Scheme 54). Concerted PCET from Ir(II) to a hydrogen-bonded complex between the ketone **54.1** and the phosphoric acid furnishes a neutral ketyl radical as a H-bonded adduct to the chiral phosphate **54.2**. The association between of the ketyl radical and the phosphate controls the enantioselectivity of the C–C bond forming step. The final product **54.4** is generated upon hydrogen atom abstraction from HEH by the hydrazyl radical **54.3**. Reduction of \*Ir(III) by HEH• affords pyridinium ion, whose subsequent deprotonation by the phosphate anion regenerates the active catalyst and completes the catalytic cycle.

In 2016, Rueping group reported that ketyl radicals generated from aromatic aldehydes under photoredox conditions can undergo an intramolecular addition to alkenes and alkynes to yield chromanol derivatives (Scheme 55).<sup>59</sup> Aldehydes containing electron-withdrawing and electron-donating substituents were well tolerated under the reaction conditions and afforded the cyclized products in modest d.r.

The authors proposed that the reaction proceeds *via* photoexcitation of Ir<sup>III</sup>(ppy)<sub>2</sub>(dtbbpy)<sup>+</sup> to \*Ir<sup>III</sup>(ppy)<sub>2</sub>(dtbbpy)<sup>+</sup>, followed by reduction of \*Ir<sup>III</sup>(ppy)<sub>2</sub>(dtbbpy)<sup>+</sup> by Hünig's base (Scheme 56). The Hünig's base cation radical **56.2** undergoes a [1,2]-H shift to form **56.3**, which is deprotonated by another molecule of **56.1** followed by oxidation to afford ammonium derivative **56.5** and iminium ion **56.6**. Either **56.5** or **56.3** can engage in a PCET with the aldehyde substrate **56.7**, facilitating its reduction by Ir<sup>II</sup>(ppy)<sub>2</sub>(dtbbpy) and formation of a neutral ketyl radical **56.8**. The ketyl radical addition to the multiple bond (6-*exo-dig* or 6-*exo-trig* cyclization) forms the chromane ring and a benzyl radical **56.9**, which abstracts a hydrogen atom to deliver the final product **56.10**.

In addition to intramolecular coupling reactions, ketyl and  $\alpha$ -aminoalkyl anion radicals generated upon a single-electron reduction of carbonyl derivatives under photoredox conditions have been reported to engage in intermolecular reactions with activated olefins. In 2016, Chen et al. reported visible-light-induced allylation and intermolecular Michael addition of aldehydes and ketones (Scheme 57).<sup>60</sup> The formation of homoallylic alcohols was achieved with iridium-based photocatalyst, Ir<sup>III</sup>(ppy)<sub>2</sub>(dtbbpy)(PF<sub>6</sub>), and when Hantzsch ester (HEH) was employed as a stoichiometric reductant. The allylation reaction proceeded efficiently with (hetero)aryl aldehydes, aryl-, ester-, and amide-substituted ketones. Michael addition of ketyl radical to (vinylsulfonyl)benzene also afforded the desired product in high yield. Aryl imines with various substitution patterns were also shown to readily participate in this polarity reversal reaction. In addition, it was demonstrated that they can undergo coupling reactions with other acceptors such as vinyl ketones, esters, and nitriles. Most



remarkably, the reaction was also applicable to alkyl imines, which were previously elusive coupling partners due to their highly negative reduction potential.<sup>106</sup> Owing to their inherent instability, alkyl imines were prepared *in situ* under the photoredox reaction conditions.

It has been proposed that the reaction proceeds as depicted in Scheme 58. Ir<sup>III</sup>(ppy)<sub>2</sub>(dtbbpy)<sup>+</sup> undergoes photoexcitation with blue light to form \*Ir<sup>III</sup>(ppy)<sub>2</sub>(dtbbpy)<sup>+</sup>. The resulting \*Ir<sup>III</sup>(ppy)<sub>2</sub>(dtbbpy)<sup>+</sup> ( $E_{1/2}^{*III/II} = +0.66$  V vs SCE)<sup>93</sup> is then reduced by Hantzsch ester to Ir<sup>II</sup>(ppy)<sub>2</sub>(dtbbpy). The highly reducing Ir<sup>II</sup>(ppy)<sub>2</sub>(dtbbpy) ( $E_{1/2}^{II/III} = -1.51$  V vs SCE)<sup>93</sup> transfers a single-electron to the aldehyde or imine activated by hydrogen bonding with Hantzsch ester cation radical (HEH<sup>•+</sup>). Following the PCET process, hydroxymethyl or  $\alpha$ -aminyl radical **58.3** undergoes addition to either the allyl sulfone **58.4** to afford the homoallylic alcohol **58.5**, or to the Michael acceptor **58.6**, to furnish the product of the Michael addition **58.7**. In this photoredox transformation, Hantzsch ester plays a dual role: it serves as electron/proton donor, and activates the aldehydes for the PCET step.

Recently, Ngai et al. disclosed a reductive coupling reaction between aldehydes and alkenylpyridines under dual Lewis acid/photoredox catalysis (Scheme 59).<sup>107</sup> The C–C bond forming event involving a ketyl radical addition to activated vinylpyridines was accomplished with Ru<sup>II</sup>(bpy)<sub>3</sub>(PF<sub>6</sub>)<sub>2</sub> as a photoredox catalyst, Hantzsch ester as a terminal reductant, and La(OTf)<sub>3</sub> as the Lewis acid activator. Under these conditions, a broad range of aryl and heteroaryl aldehydes, including complex substrates, were readily converted into secondary alcohols in high yields. With respect to the alkenylpyridine coupling partners the reaction tolerated a wide scope of substituents at the  $\alpha$ -position of alkenylpyridines, including hydrogen atom, alkyl group, as well as aromatic and heteroaromatic moieties. The corresponding coupling products were obtained in good to excellent yields and with modest diastereoselectivities. In addition to ketyl radicals,  $\alpha$ -aminoalkyl anion radicals generated from aromatic imines upon a SET were reported to undergo the coupling reaction with 4-vinylpyridine. The reaction was observed to proceed well regardless of the electronic structure of the iminyl aromatic rings.

The proposed mechanistic details of the coupling reaction are depicted in Scheme 60. Irradiation of Ru(bpy)<sub>3</sub><sup>2+</sup> with visible light produces a long-lived (1.1  $\mu$ s)<sup>108</sup> photoexcited state, \*Ru<sup>II</sup>(bpy)<sub>3</sub><sup>2+</sup>, which is then reduced by the catalytically generated intermediate Hantzsch ester radical (HEH<sup>•</sup>) to form a strongly reducing ruthenium (I) species, Ru<sup>I</sup>(bpy)<sub>3</sub><sup>+</sup>, and pyridinium ion PyH<sup>+</sup>. Ru(bpy)<sub>3</sub><sup>+</sup> ( $E_{1/2}^{red} = -1.33$  V vs SCE)<sup>66</sup> subsequently participates in a PCET with the aldehyde activated by hydrogen bonding with PyH<sup>+</sup> (**60.1**) to afford ketyl radical intermediate **60.2** and regenerate the Ru<sup>I</sup>(bpy)<sub>3</sub><sup>2+</sup> catalyst. Radical **60.2** adds to Lewis acid-activated 4-vinylpyridine **60.4** to form radical **60.5**, which abstracts a hydrogen atom from HEH, generating the Lewis acid-bounded product **60.6** and another molecule of a reductant (HEH<sup>•</sup>) capable of reducing \*Ru<sup>II</sup>(bpy)<sub>3</sub><sup>2+</sup>. Replacement of the product by new 4-vinylpyridine **60.3** substrate liberates the desired coupling product **60.7** and completes the catalytic cycle.

## Conclusions and Future Outlook

Recent years have witnessed a tremendous progress in reactions of carbonyl derivatives initiated by a SET from organometallic photoredox catalysts. Generation of ketyl and  $\alpha$ -aminyl anion radicals from aldehydes, ketones, and imines under photochemical conditions has obviated the need for strong stoichiometric reductants, and provided an access to important synthons under mild reaction conditions using simple reagents and catalysts. Moreover, it has enabled a variety of transformations that would otherwise be difficult or even impossible to achieve. A number of these photoredox reactions tolerate a wide array of functional groups, facilitate novel reactivities (e.g.  $\beta$ -functionalization of ketones), and allow the synthesis of medically-relevant compounds and structures of unprecedented molecular architectures. Recently described catalytic enantioselective reactions that rely on the use of a chiral catalyst have provided means for precise stereocontrol over the reactivity of ion-radicals and significantly advanced the field of asymmetric radical chemistry. With the continuing interest of the scientific community in photoredox catalysis, one might expect to see further applications of the photocatalytically-generated ketyl and  $\alpha$ -aminyl anion radicals in synthesis.

## Acknowledgments

We thank National Institute of General Medical Sciences (R35GM119652) and start-up funds from Stony Brook University for supporting our research. K.N.L. received the graduate fellowship from the NIH Chemical-Biology training grant (T32GM092714). The content is solely the responsibility of the authors and does not necessarily represent the official views of the National Institutes of Health.

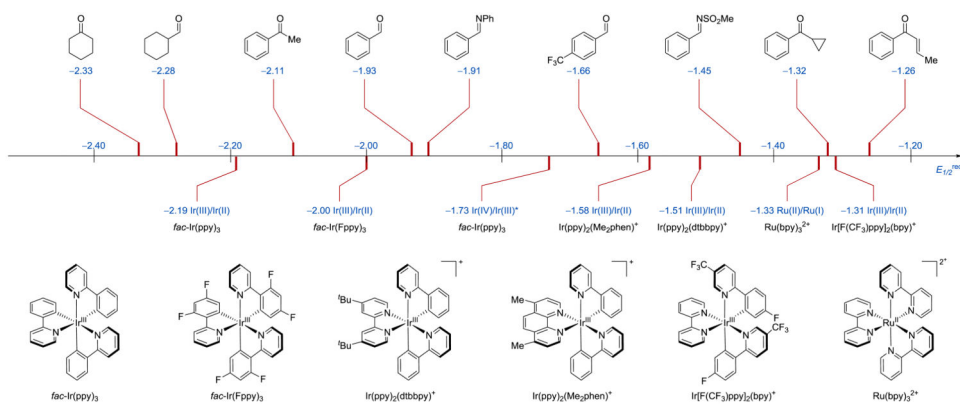
## References

1. Corey EJ. *Pure Appl Chem.* 1967; 14:19–37.
2. Seebach D. *Angew Chem Int Ed.* 1979; 18:239–258.
3. Nicolaou KC, Ellery SP, Chen JS. *Angew Chem Int Ed.* 2009; 48:7140–7165.
4. Reduction potentials provided in this Review were reported against SCE in MeCN unless otherwise stated. When a reduction potential was reported against a different electrode in the original reference, the reduction potential against SCE was calculated by using the conversion factor described in the following reference: Pavlishchuk VV, Addison AW. *Inorg Chim Acta.* 2000; 298:97–102.
5. Roth HG, Romero NA, Nicewicz DA. *Synlett.* 2016; 27:714–723.
6. Pradhan SK, Kadam SR, Kolhe JN, Radhakrishnan TV, Sohani SV, Thaker VB. *J Org Chem.* 1981; 46:2622–2633.
7. Ikeda T, Yue S, Hutchinson CR. *J Org Chem.* 1985; 50:5193–5199.
8. Beckwith ALJ, Roberts DH. *J Am Chem Soc.* 1986; 108:5893–5901. [PubMed: 22175347]
9. Ardisson J, Férézou JP, Julia M, Pancrazi A. *Tetrahedron Lett.* 1987; 28:2001–2003.
10. Sugawara T, Otter BA, Ueda T. *Tetrahedron Lett.* 1988; 29:75–78.
11. Enholm EJ, Prasad G. *Tetrahedron Lett.* 1989; 30:4939–4942.
12. Enholm EJ, Burroff JA. *Tetrahedron Lett.* 1992; 33:1835–1838.
13. Hays DS, Fu GC. *J Org Chem.* 1996; 61:4–5.
14. Corey EJ, Pyne SG. *Tetrahedron Lett.* 1983; 24:2821–2824.
15. Yeh CH, Korivi RP, Cheng CH. *Adv Synth Catal.* 2013; 355:1338–1344.
16. Estévez RE, Oller-López JL, Robles R, Melgarejo CR, Gansäuer A, Cuerva JM, Oltra JE. *Org Lett.* 2006; 8:5433–5436. [PubMed: 17107040]
17. Elango TP, Ramakrishnan V, Vancheesan S, Kuriacose JC. *Tetrahedron.* 1985; 41:3837–3843.

18. Fukuzawa S, Nakanishi A, Fujinami T, Sakai S. *J Chem Soc Chem Comm.* 1986; 0:624–625.
19. Otsubo K, Inanaga J, Yamaguchi M. *Tetrahedron Lett.* 1986; 27:5763–5764.
20. Molander GA, Kenny C. *Tetrahedron Lett.* 1987; 28:4367–4370.
21. Molander GA, Kenny C. *J Am Chem Soc.* 1989; 111:8236–8246.
22. Mikami K, Yamaoka M. *Tetrahedron Lett.* 1998; 39:4501–4504.
23. Froling A. *Recl Trav Chim Pays Bas.* 1974; 93:47–51.
24. Shono T, Nishiguchi I, Omizu H. *Chem Lett.* 1976; 5:1233–1236.
25. Shono T, Ohmizu H, Kawakami S, Sugiyama H. *Tetrahedron Lett.* 1980; 21:5029–5032.
26. Shono T, Kashimura S, Mori Y, Hayashi T, Soejima T, Yamaguchi Y. *J Org Chem.* 1989; 54:6001–6003.
27. Belotti D, Cossy J, Pete JP, Portella C. *Tetrahedron Lett.* 1985; 26:4591–4594.
28. Belotti D, Cossy J, Pete JP, Portella C. *J Org Chem.* 1986; 51:4196–4200.
29. Cossy J, Belotti D, Pete JP. *Tetrahedron Lett.* 1987; 28:4547–4550.
30. Cossy J, Pete JP, Portella C. *Tetrahedron Lett.* 1989; 30:7361–7364.
31. Cossy J, Belotti D, Cuong NK, Chassagnard C. *Tetrahedron.* 1993; 49:7691–7700.
32. Cossy J, Belotti D. *Tetrahedron.* 2006; 62:6459–6470.
33. Hirao T. *Top Curr Chem.* 2007; 279:53–75.
34. Streuff J. *Synthesis-Stuttgart.* 2013; 45:281–307.
35. Castro Rodríguez M, Rodríguez García I, Rodríguez Maecker RN, Pozo Morales L, Oltra JE, Rosales Martínez A. *Org Process Res Dev.* 2017; 21:911–923.
36. Frey G, Hausmann JN, Streuff J. *Chem Eur J.* 2015; 21:5693–5696. [PubMed: 25712472]
37. Saito T, Nishiyama H, Tanahashi H, Kawakita K, Tsurugi H, Mashima K. *J Am Chem Soc.* 2014; 136:5161–5170. [PubMed: 24597916]
38. Morcillo SP, Miguel D, Campana AG, Alvarez de Cienfuegos L, Justicia J, Cuerva JM. *Org Chem Front.* 2014; 1:15–33.
39. Skubi KL, Blum TR, Yoon TP. *Chem Rev.* 2016; 116:10035–10074. [PubMed: 27109441]
40. Shaw MH, Twilton J, MacMillan DWC. *J Org Chem.* 2016; 81:6898–6926. [PubMed: 27477076]
41. Romero NA, Nicewicz DA. *Chem Rev.* 2016; 116:10075–10166. [PubMed: 27285582]
42. Kärkäs MD, Porco JA, Stephenson CRJ. *Chem Rev.* 2016; 116:9683–9747. [PubMed: 27120289]
43. Prier CK, Rankic DA, MacMillan DWC. *Chem Rev.* 2013; 113:5322–5363. [PubMed: 23509883]
44. Hedstrand DM, Kruizinga WH, Kellogg RM. *Tetrahedron Lett.* 1978; 19:1255–1258.
45. Fukuzumi S, Ishikawa K, Hironaka K, Tanaka T. *J Chem Soc Perk T 2.* 1987; 0:751–760.
46. Shibata T, Kabumoto A, Shiragami T, Ishitani O, Pac C, Yanagida S. *J Phys Chem.* 1990; 94:2068–2076.
47. Ischay MA, Anzovino ME, Du J, Yoon TP. *J Am Chem Soc.* 2008; 130:12886–12887. [PubMed: 18767798]
48. Du J, Yoon TP. *J Am Chem Soc.* 2009; 131:14604–14605. [PubMed: 19473018]
49. Du JN, Espelt LR, Guzei IA, Yoon TP. *Chem Sci.* 2011; 2:2115–2119. [PubMed: 22121471]
50. Hurlley AE, Cismesia MA, Ischay MA, Yoon TR. *Tetrahedron.* 2011; 67:4442–4448. [PubMed: 21666769]
51. Zhang M, Rouch WD, McCulla RD. *Eur J Org Chem.* 2012:6187–6196.
52. Petronijevic FR, Nappi M, MacMillan DWC. *J Am Chem Soc.* 2013; 135:18323–18326. [PubMed: 24237366]
53. Rono LJ, Yayla HG, Wang DY, Armstrong MF, Knowles RR. *J Am Chem Soc.* 2013; 135:17735–17738. [PubMed: 24215561]
54. Tarantino KT, Liu P, Knowles RR. *J Am Chem Soc.* 2013; 135:10022–10025. [PubMed: 23796403]
55. Du JN, Skubi KL, Schultz DM, Yoon TP. *Science.* 2014; 344:392–396. [PubMed: 24763585]
56. Nakajima M, Fava E, Loescher S, Jiang Z, Rueping M. *Angew Chem Int Ed.* 2015; 54:8828–8832.

57. Amador AG, Sherbrook EM, Yoon TP. *J Am Chem Soc.* 2016; 138:4722–4725. [PubMed: 27015009]
58. Fava E, Millet A, Nakajima M, Loescher S, Rueping M. *Angew Chem Int Ed Engl.* 2016; 55:6776–6779. [PubMed: 27136443]
59. Fava E, Nakajima M, Nguyen ALP, Rueping M. *J Org Chem.* 2016; 81:6959–6964. [PubMed: 27442851]
60. Qi L, Chen YY. *Angew Chem Int Ed.* 2016; 55:13312–13315.
61. Larraufie MH, Pellet R, Fensterbank L, Goddard JP, Lacote E, Malacria M, Ollivier C. *Angew Chem Int Ed.* 2011; 50:4463–4466.
62. Wang C, Qin J, Shen X, Riedel R, Harms K, Meggers E. *Angew Chem Int Ed.* 2016; 55:685–688.
63. Jeffrey JL, Petronijevi FR, MacMillan DWC. *J Am Chem Soc.* 2015; 137:8404–8407. [PubMed: 26075347]
64. Uraguchi D, Kinoshita N, Kizu T, Ooi T. *J Am Chem Soc.* 2015; 137:13768–13771. [PubMed: 26456298]
65. Fuentes de Arriba AL, Urbitsch F, Dixon DJ. *Chem Commun.* 2016; 52:14434–14437.
66. Kalyanasundaram K. *Coord Chem Rev.* 1982; 46:159–244.
67. Huynh MHV, Meyer TJ. *Chem Rev.* 2007; 107:5004–5064. [PubMed: 17999556]
68. Reduction potentials of the compounds cited in the schemes are obtained from the following references: Cyclopropylketone: Mandell L, Johnston JC, Day RA. *J Org Chem.* 1978; 43:1616–1618. Enone: Roh Y, Jang HY, Lynch V, Bauld NL, Krische MJ. *Org Lett.* 2002; 4:611–613. [PubMed: 11843604] Carbonyl compounds: reference #5. N-Benzylidenemethanesulfonamide: reference #64. Reduction potentials of photoredox catalyst were taken from the references cited throughout the Review.
69. Mayer JM. *Annu Rev Phys Chem.* 2004; 55:363–390. [PubMed: 15117257]
70. Weinberg DR, Gagliardi CJ, Hull JF, Murphy CF, Kent CA, Westlake BC, Paul A, Ess DH, McCafferty DG, Meyer TJ. *Chem Rev.* 2012; 112:4016–4093. [PubMed: 22702235]
71. Yayla HG, Knowles RR. *Synlett.* 2014; 25:2819–2826.
72. Roughley SD, Jordan AM. *J Med Chem.* 2011; 54:3451–3479. [PubMed: 21504168]
73. Van Bergen TJ, Hedstrand DM, Kruizinga WH, Kellogg RM. *J Org Chem.* 1979; 44:4953–4962.
74. Ono N, Tamura R, Kaji A. *J Am Chem Soc.* 1980; 102:2851–2852.
75. Nakamura K, Fujii M, Mekata H, Oka S, Ohno A. *Chem Lett.* 1986; 15:87–88.
76. Tanner DD, Singh HK, Kharrat A, Stein AR. *J Org Chem.* 1987; 52:2142–2146.
77. Fukuzumi S, Mochizuki S, Tanaka T. *J Phys Chem.* 1990; 94:722–726.
78. Narayanam JMR, Tucker JW, Stephenson CRJ. *J Am Chem Soc.* 2009; 131:8756–8757. [PubMed: 19552447]
79. Fukuzumi S, Koumitsu S, Hironaka K, Tanaka T. *J Am Chem Soc.* 1987; 109:305–316.
80. Boujlel K, Martigny P, Simonet J. *J Electroanal Chem Interfacial Electrochem.* 1983; 144:437–442.
81. Chen WX, Liu Z, Tian JQ, Li J, Ma J, Cheng X, Li GG. *J Am Chem Soc.* 2016; 138:12312–12315. [PubMed: 27622653]
82. Zhu XQ, Li HR, Li Q, Ai T, Lu JY, Yang Y, Cheng JP. *Chem Eur J.* 2003; 9:871–880. [PubMed: 12584702]
83. Sim BA, Griller D, Wayner DDM. *J Am Chem Soc.* 1989; 111:754–755.
84. Flamigni, L., Barbieri, A., Sabatini, C., Ventura, B., Barigelletti, F. *Photochemistry and Photophysics of Coordination Compounds II.* Balzani, V., Campagna, S., editors. Vol. 281. Springer Berlin Heidelberg; Berlin, Heidelberg; 2007. p. 143-203.
85. Dange NS, Hussain Jatoi A, Robert F, Landais Y. *Org Lett.* 2017; 19:3652–3655. [PubMed: 28656767]
86. Dixon IM, Collin JP, Sauvage JP, Flamigni L, Encinas S, Barigelletti F. *Chem Soc Rev.* 2000; 29:385–391.
87. Ishitani O, Pac C, Sakurai H. *J Org Chem.* 1983; 48:2941–2942.
88. Ishitani O, Yanagida S, Takamuku S, Pac C. *J Org Chem.* 1987; 52:2790–2796.
89. Ishitani O, Pac C, Sakurai H. *J Org Chem.* 1983; 48:2941–2942.

90. Wagner PJ, Truman RJ, Puchalski AE, Wake R. *J Am Chem Soc.* 1986; 108:7727–7738. [PubMed: 22283279]
91. Schoeller WW, Niemann J, Rademacher P. *J Chem Soc Perk T 2.* 1988; 0:369–373.
92. Lowry MS, Goldsmith JI, Slinker JD, Rohl R, Pascal RA, Malliaras GG, Bernhard S. *Chem Mater.* 2005; 17:5712–5719.
93. Pischel U, Zhang X, Hellrung B, Haselbach E, Muller PA, Nau WM. *J Am Chem Soc.* 2000; 122:2027–2034.
94. Hager D, MacMillan DWC. *J Am Chem Soc.* 2014; 136:16986–16989. [PubMed: 25457231]
95. Slinker JD, Gorodetsky AA, Lowry MS, Wang J, Parker S, Rohl R, Bernhard S, Malliaras GG. *J Am Chem Soc.* 2004; 126:2763–2767. [PubMed: 14995193]
96. Ma JJ, Harms K, Meggers E. *Chem Commun.* 2016; 52:10183–10186.
97. Cooper BE, Owen WJ. *J Organomet Chem.* 1971; 29:33–40.
98. Chen M, Zhao X, Yang C, Xia W. *Org Lett.* 2017; 19:3807–3810. [PubMed: 28696124]
99. Tyson EL, Farney EP, Yoon TP. *Org Lett.* 2012; 14:1110–1113. [PubMed: 22320352]
100. House HO, Huber LE, Umen MJ. *J Am Chem Soc.* 1972; 94:8471–8475.
101. Lu Z, Shen M, Yoon TP. *J Am Chem Soc.* 2011; 133:1162–1164. [PubMed: 21214249]
102. Zhao G, Yang C, Guo L, Sun H, Lin R, Xia W. *J Org Chem.* 2012; 77:6302–6306. [PubMed: 22731518]
103. Zhou Z, Li Y, Han B, Gong L, Meggers E. *Chem Sci.* 2017; 8:5757–5763. [PubMed: 28989615]
104. Yuan W, Zhou Z, Gong L, Meggers E. *Chem Commun.* 2017; 53:8964–8967.
105. Kunai A, Harada J, Nishihara M, Yanagi Y, Sasaki K. *Bull Chem Soc Jpn.* 1983; 56:2442–2446.
106. Lee KN, Lei Z, Ngai MY. *J Am Chem Soc.* 2017; 139:5003–5006.
107. Juris A, Balzani V, Belser P, von Zelewsky A. *Helv Chim Acta.* 1981; 64:2175–2182.

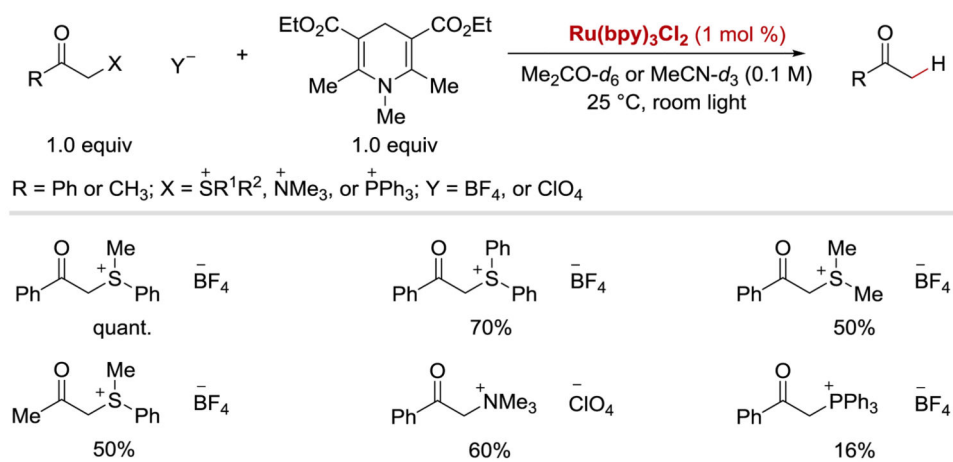


### Scheme 1.

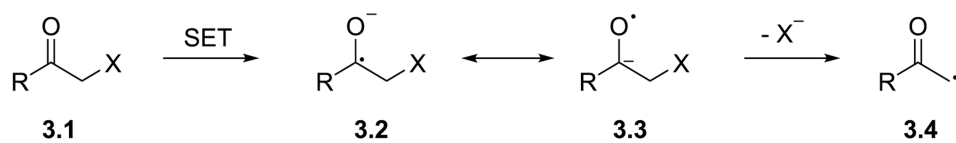
Electrochemical series of selected carbonyl derivatives; potentials are reported against SCE.

68

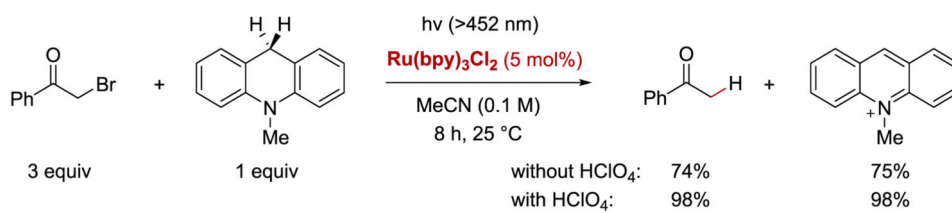


**Scheme 2.**

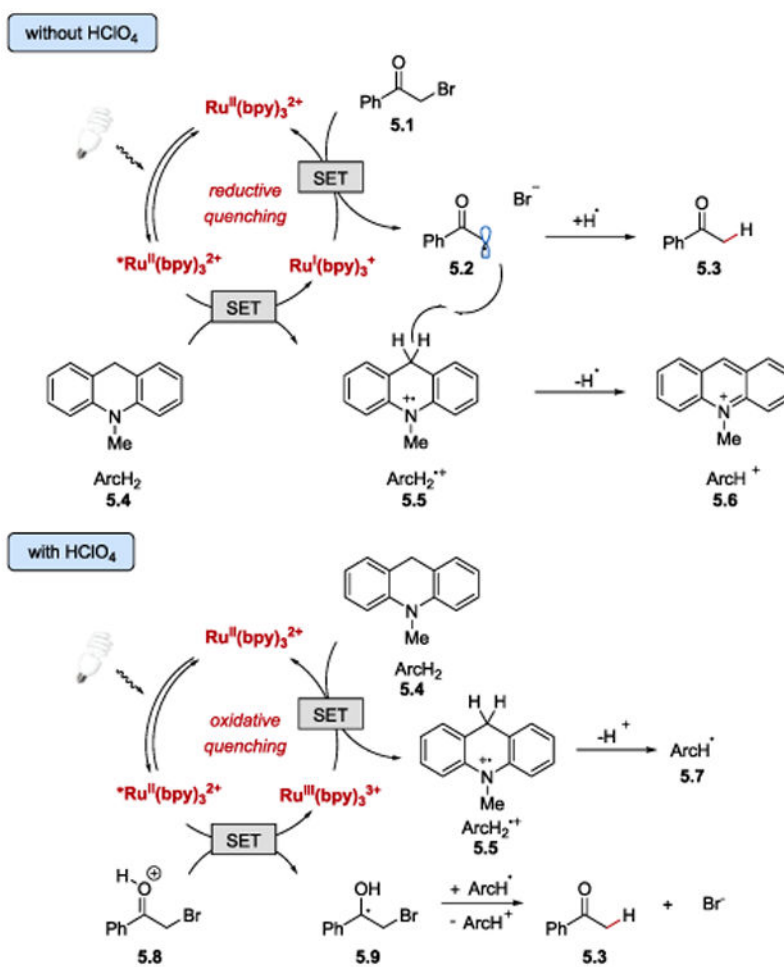
Photoredox-catalysed reduction of phenacyl onium salts with *N*-substituted 1,4-dihydropyridines.



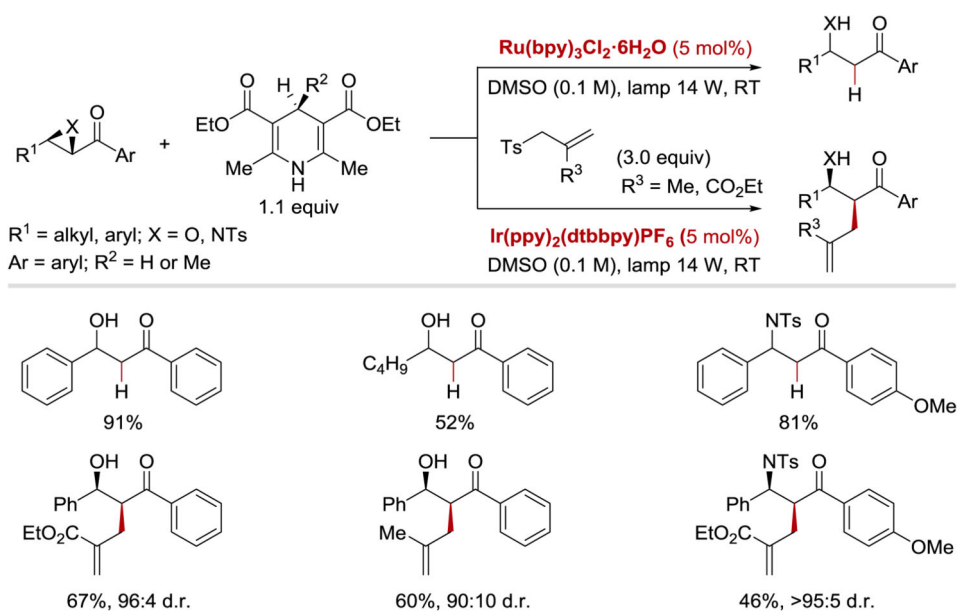
**Scheme 3.**  
Proposed mechanism for a single-electron reduction of  $\alpha$ -heteroatom substituted carbonyl compounds.



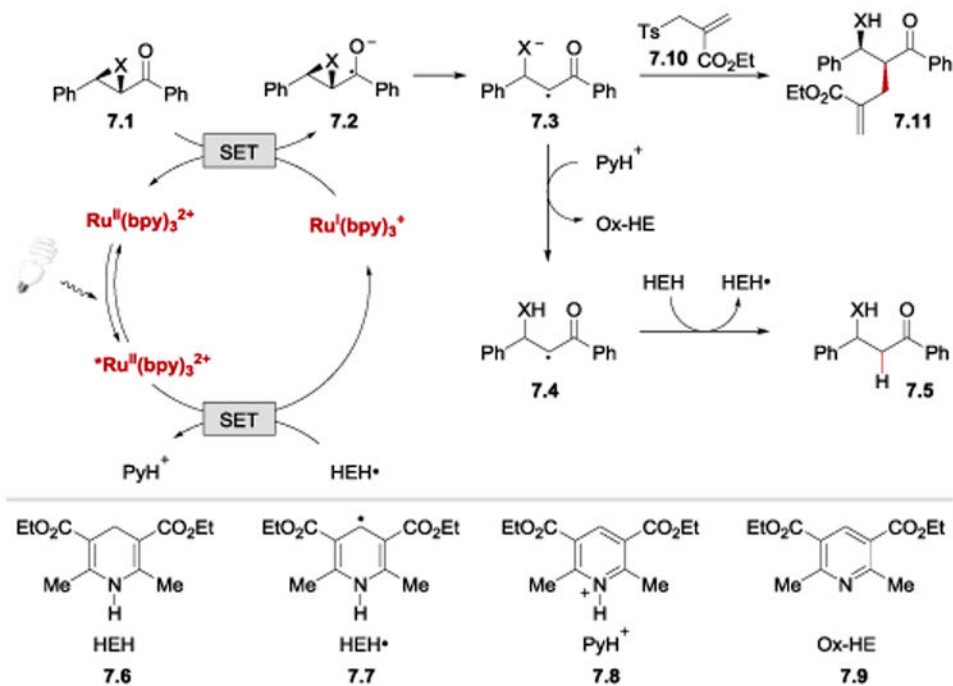
**Scheme 4.**  
Reductive dehalogenation of phenacyl bromides in the absence and presence of an acid additive.<sup>77</sup>



**Scheme 5.** Electron transfer pathways in photoredox reduction of phenacyl halides by dihydroacridine derivatives with and without perchloric acid.<sup>77</sup>

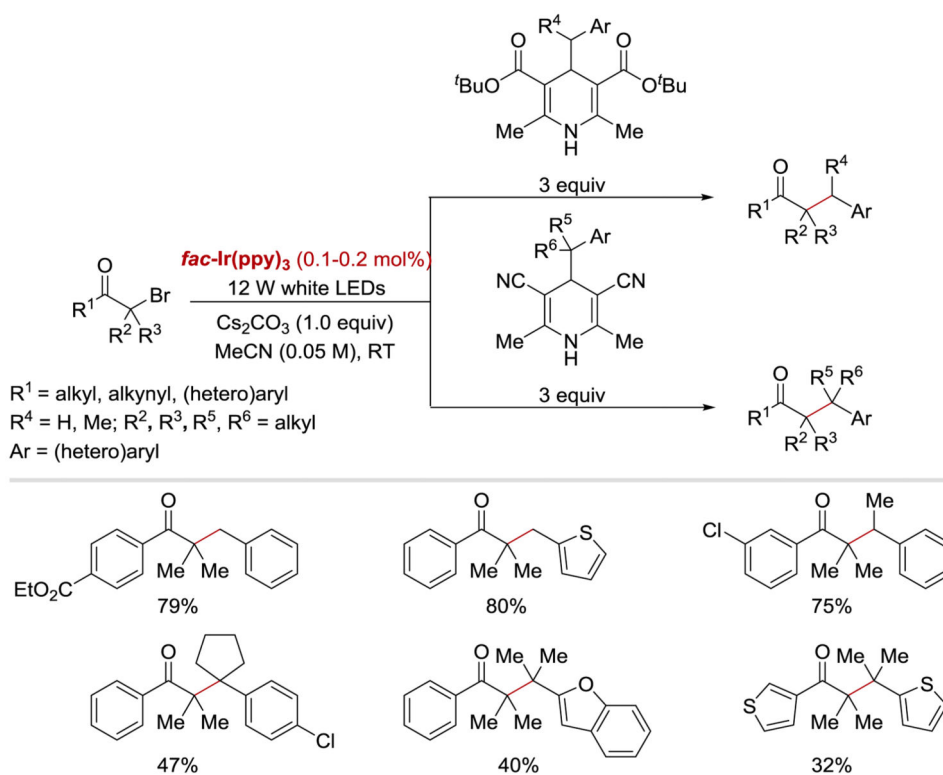


**Scheme 6.** Photocatalytic reductive ring opening of epoxides and aziridines and reductive allylation reaction.<sup>61</sup>

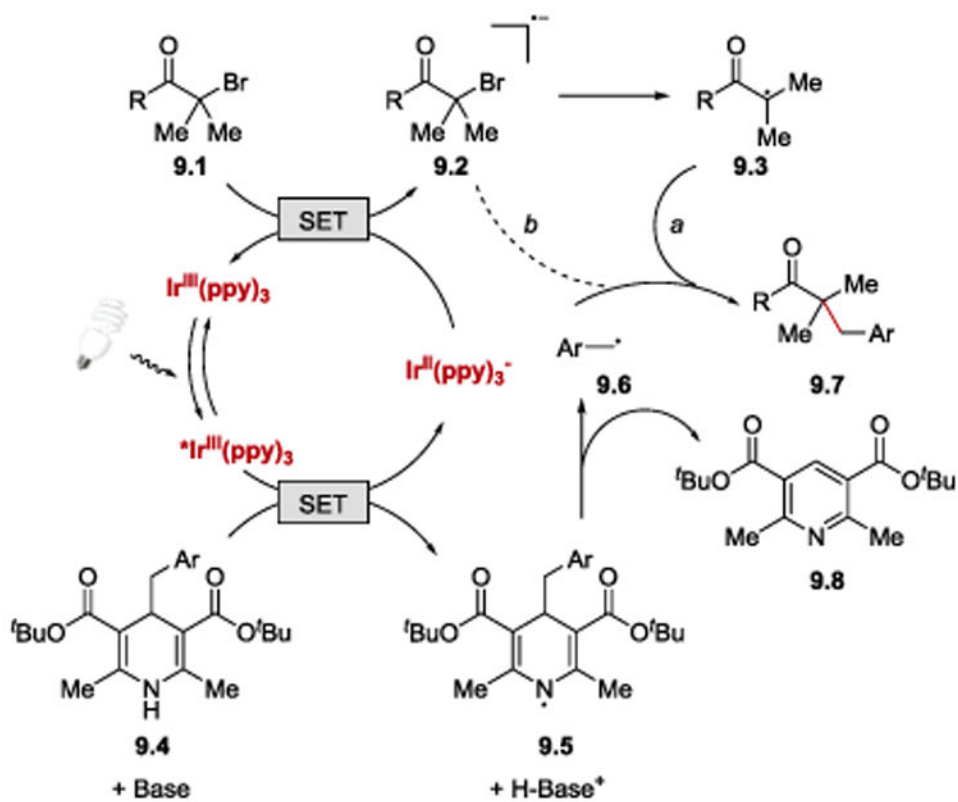
**Scheme 7.**

Plausible mechanism of the photocatalytic reductive ring opening of epoxides and aziridines and reductive allylation.<sup>61, 81</sup>

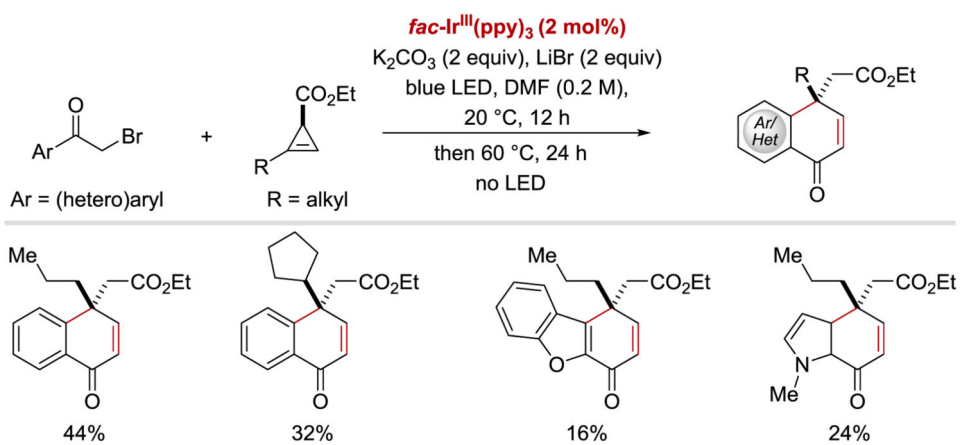


**Scheme 8.**

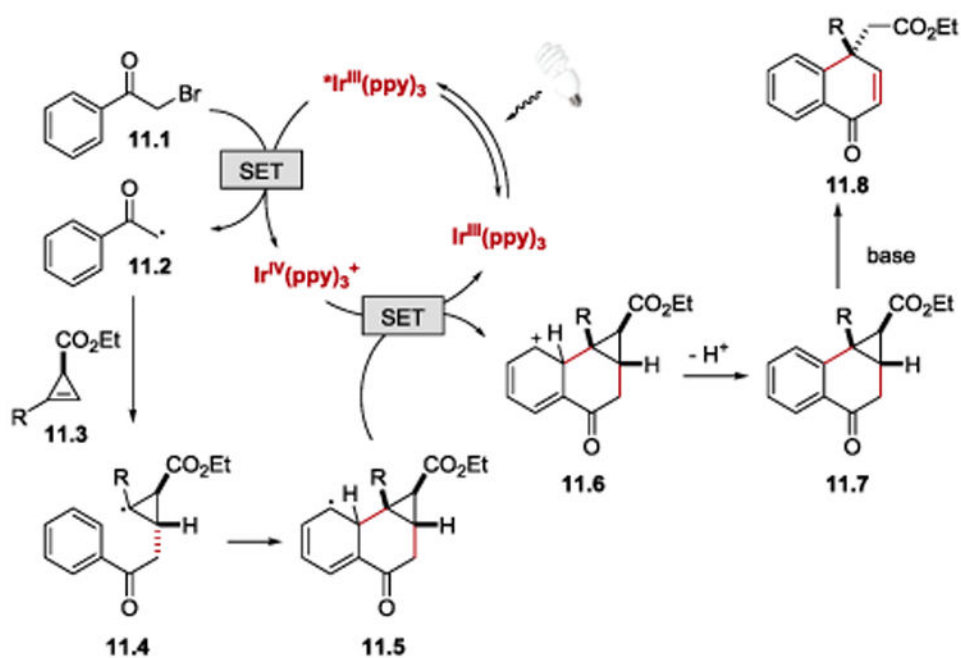
Photoredox catalyzed synthesis of congested ketones with 4-alkyl Hantzsch esters and 4-alkyl Hantzsch nitriles as precursors for alkyl radicals.<sup>82</sup>



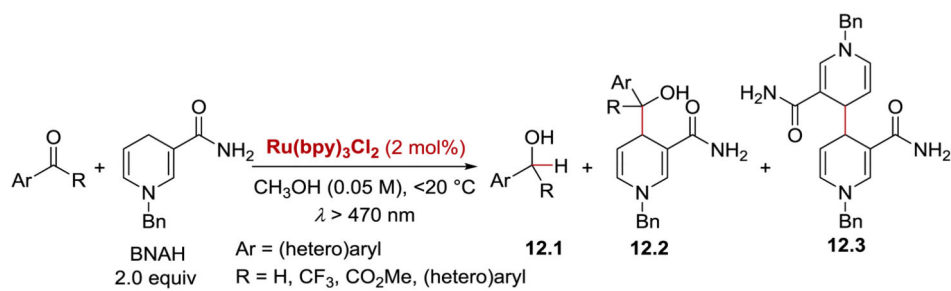
**Scheme 9.**  
Proposed mechanism of the visible-light photoredox transfer alkylation reaction.<sup>82</sup>



**Scheme 10.**  
 Photoredox-catalysed intramolecular carboarylation of cyclopropenes.<sup>86</sup>

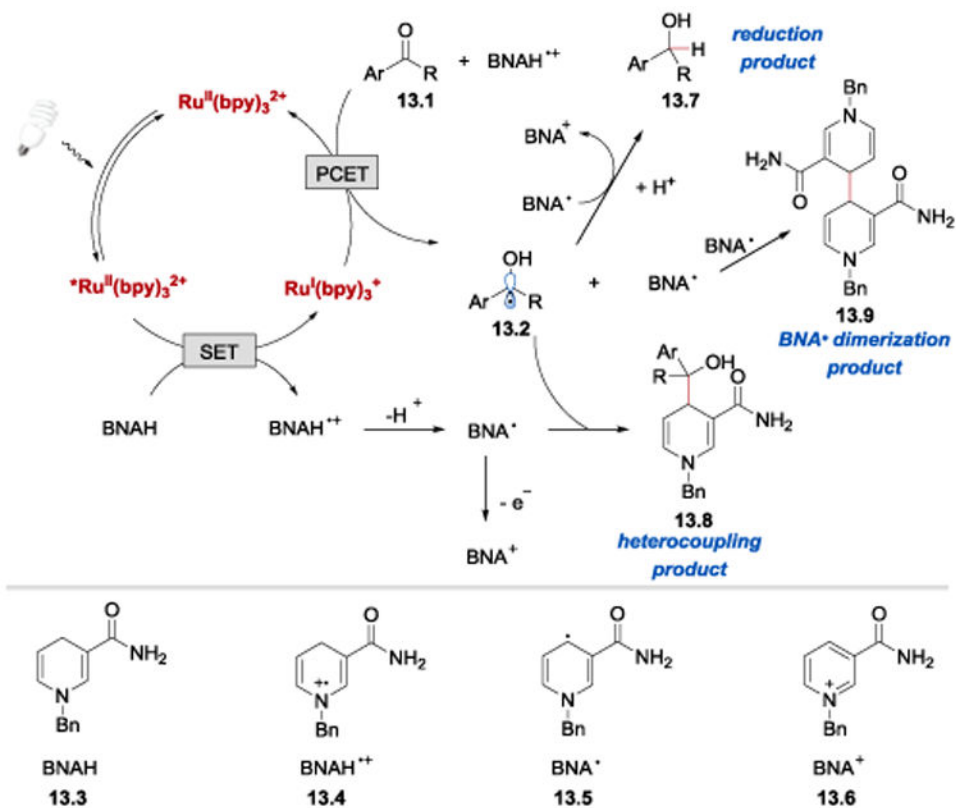
**Scheme 11.**

Proposed mechanism for the photoredox-catalysed reaction between phenacyl bromides and cyclopropenes.<sup>86</sup>



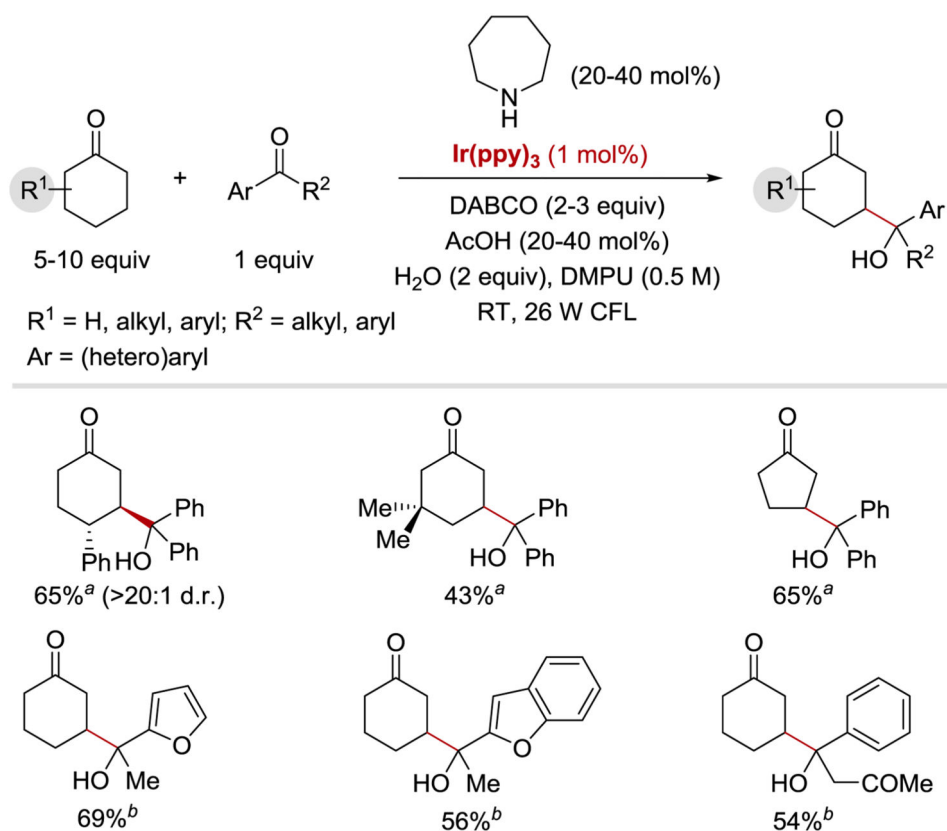
Substrate	Isolated Yield		
	12.1	12.2	12.3 <sup>a</sup>
	0	85%	<1%
	16%	56%	8%
	20%	33%	53%
	<4%	44%	9%
	>90%	0%	50%

**Scheme 12.** Ru(bpy)<sub>3</sub><sup>2+</sup>-catalysed reactions of carbonyl compounds with BNAH. <sup>a</sup>Yield based on BNAH used.<sup>88</sup>



Scheme 13.

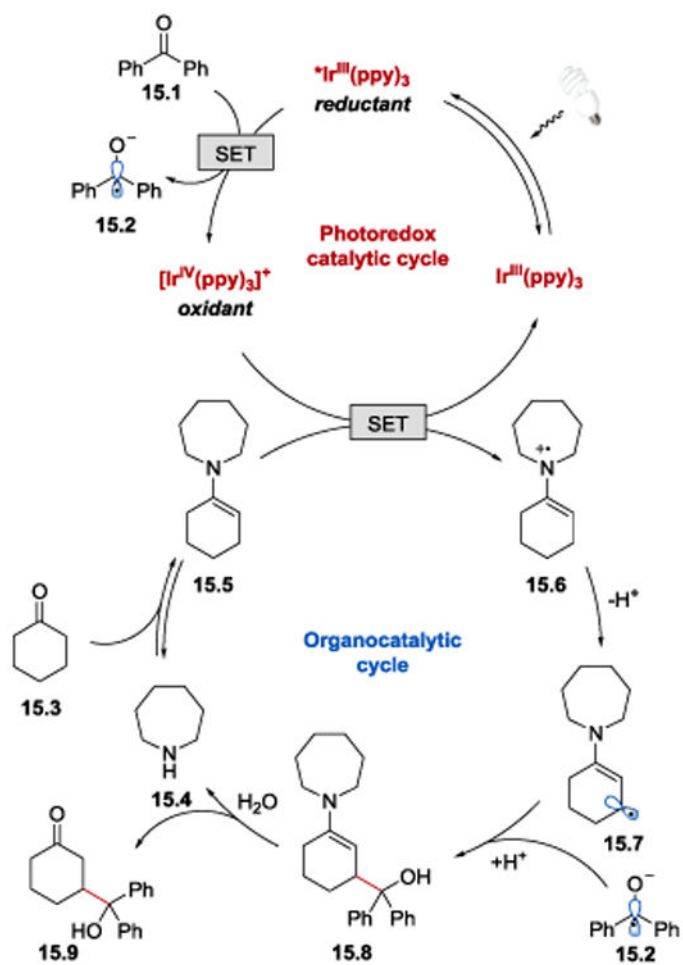
Proposed mechanism of the photoredox-catalysed transformations of carbonyl compounds with BNAH.<sup>88-90</sup>

**Scheme 14.**

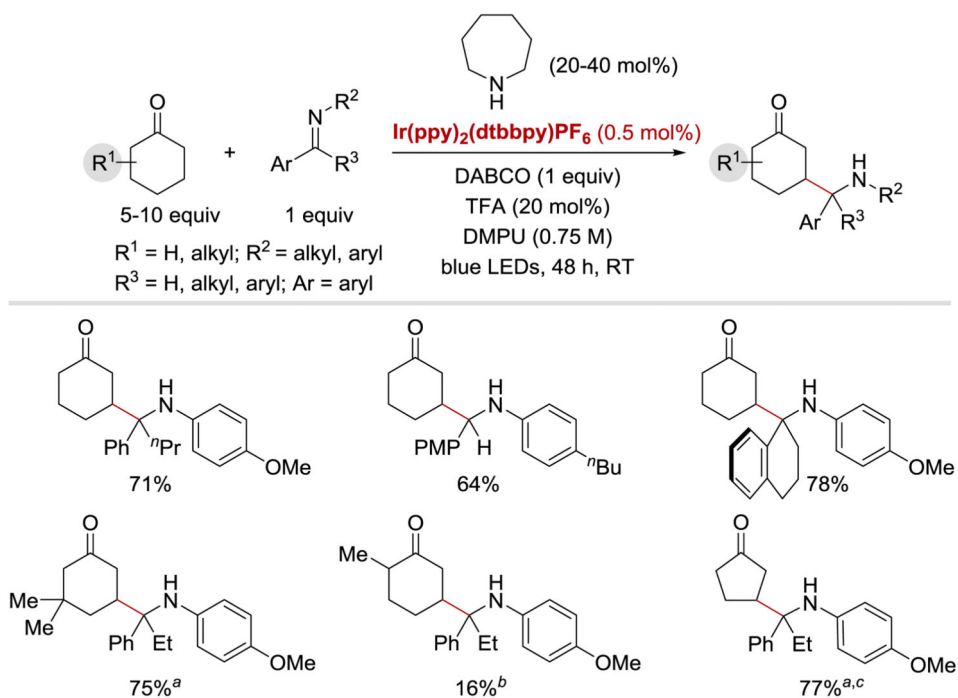
Direct  $\beta$ -functionalization of cyclic ketones with biaryl and aryl-alkyl ketones *via* the merger of photoredox and organocatalysis. <sup>a</sup>Reaction performed with 1.0 equiv of LiAsF<sub>6</sub>.

<sup>b</sup>Reaction performed with Ir(*p*-OMe-ppy)<sub>3</sub>, in MeCN (0.17 M).<sup>52</sup>

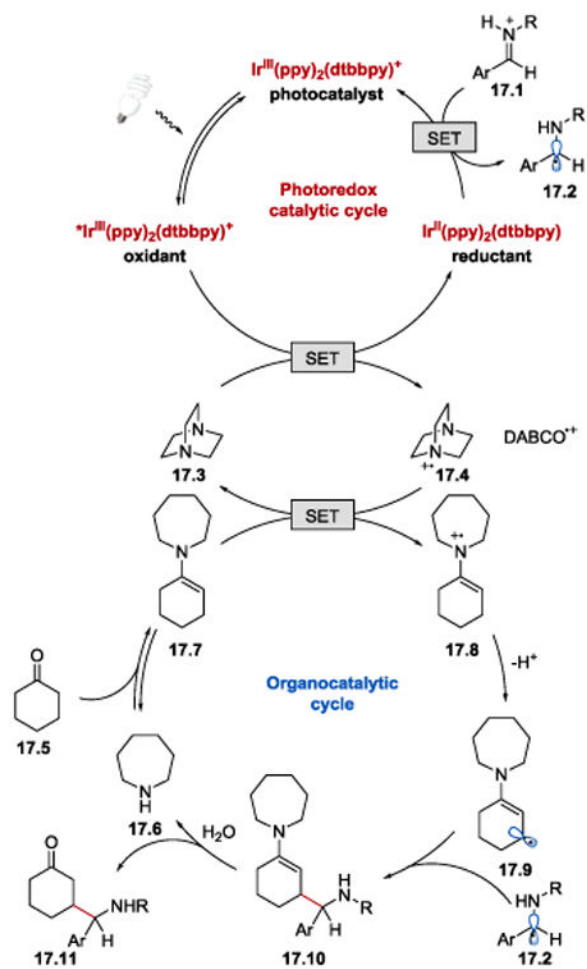




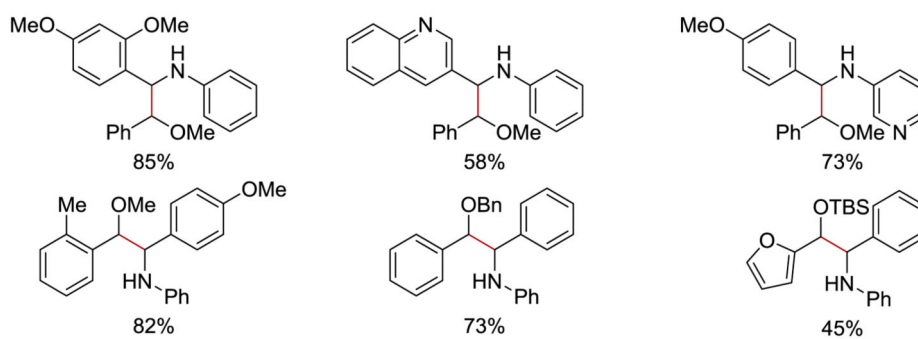
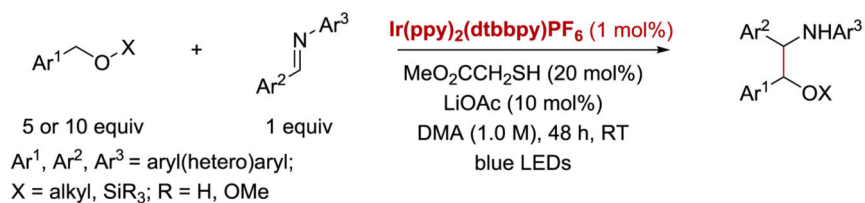
**Scheme 15.** Proposed mechanism for the synthesis of  $\gamma$ -hydroxyketones under photoredox conditions.<sup>52</sup>

**Scheme 16.**

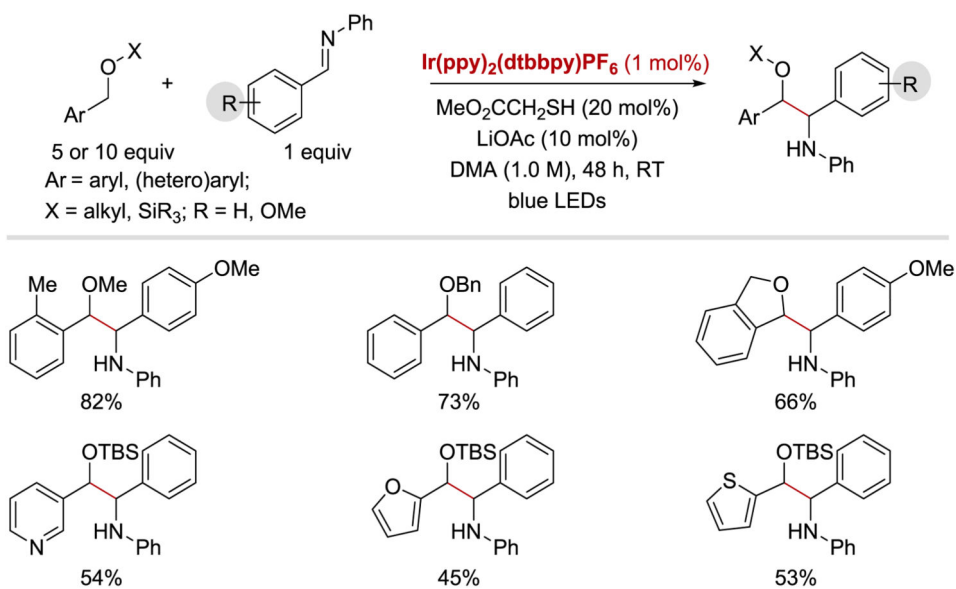
Photoredox-catalysed synthesis of  $\gamma$ -aminoketones. Diastereomeric ratios were between 1:1 and 1.5:1. <sup>a</sup>LiBF<sub>4</sub> (1.0 equiv) was added. <sup>b</sup>Pyrrolidine (20 mol%) was used in place of azepane. <sup>c</sup>Morpholine (40 mol%) was used in place of azepane.<sup>63</sup>



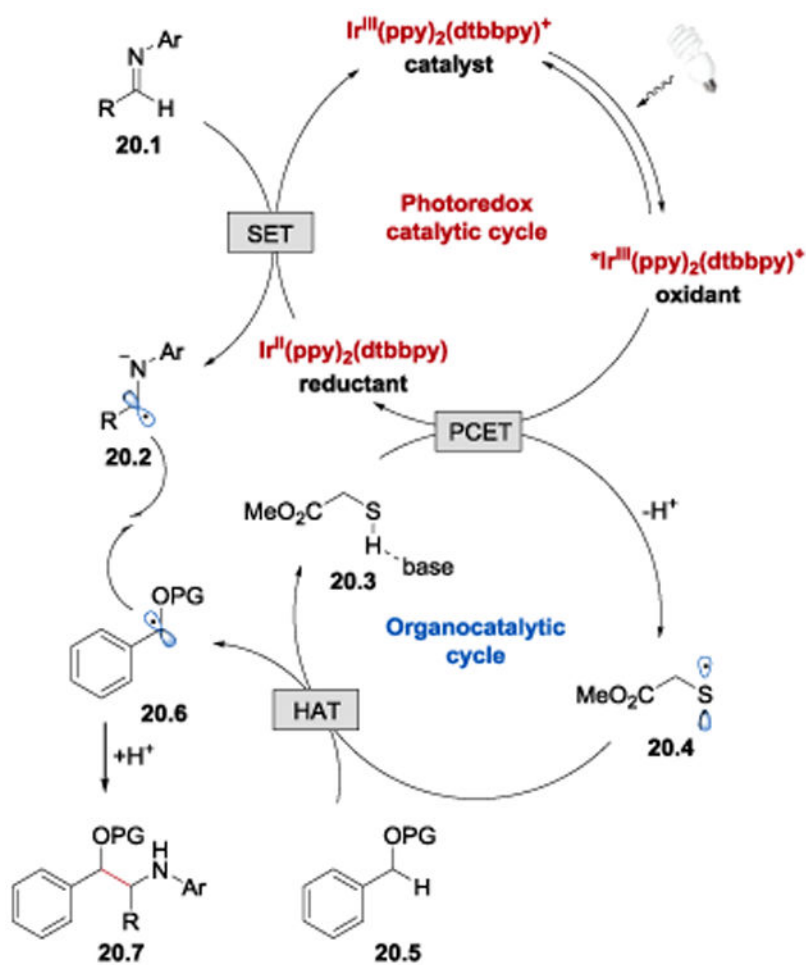
**Scheme 17.** Proposed mechanism for the synthesis of  $\gamma$ -aminoketones under photoredox conditions.<sup>63</sup>

**Scheme 18.**

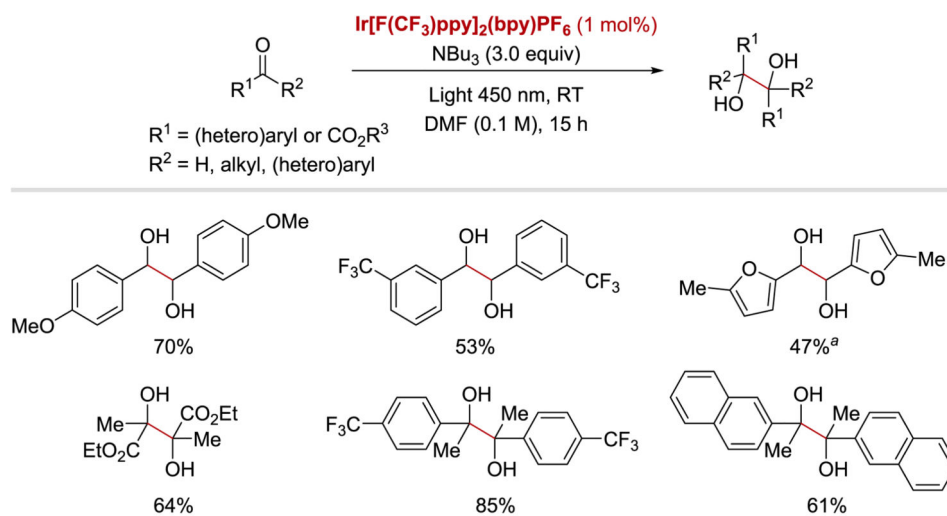
Coupling of benzylic ethers with imines: imine substrate scope.<sup>95</sup>



**Scheme 19.**  
Coupling of benzylic ethers with imines: ether substrate scope.<sup>95</sup>

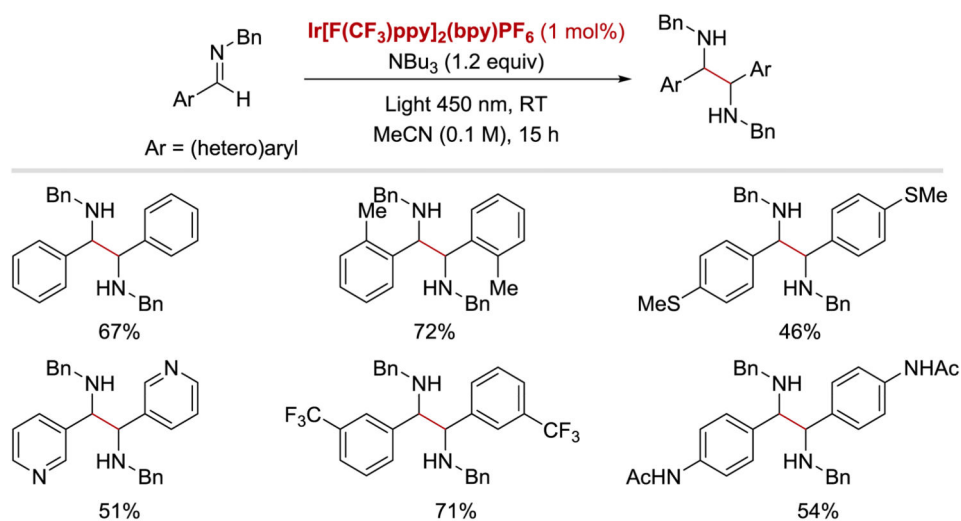


**Scheme 20.** Proposed mechanism of the coupling reaction between benzylic ethers and imines.<sup>95</sup>

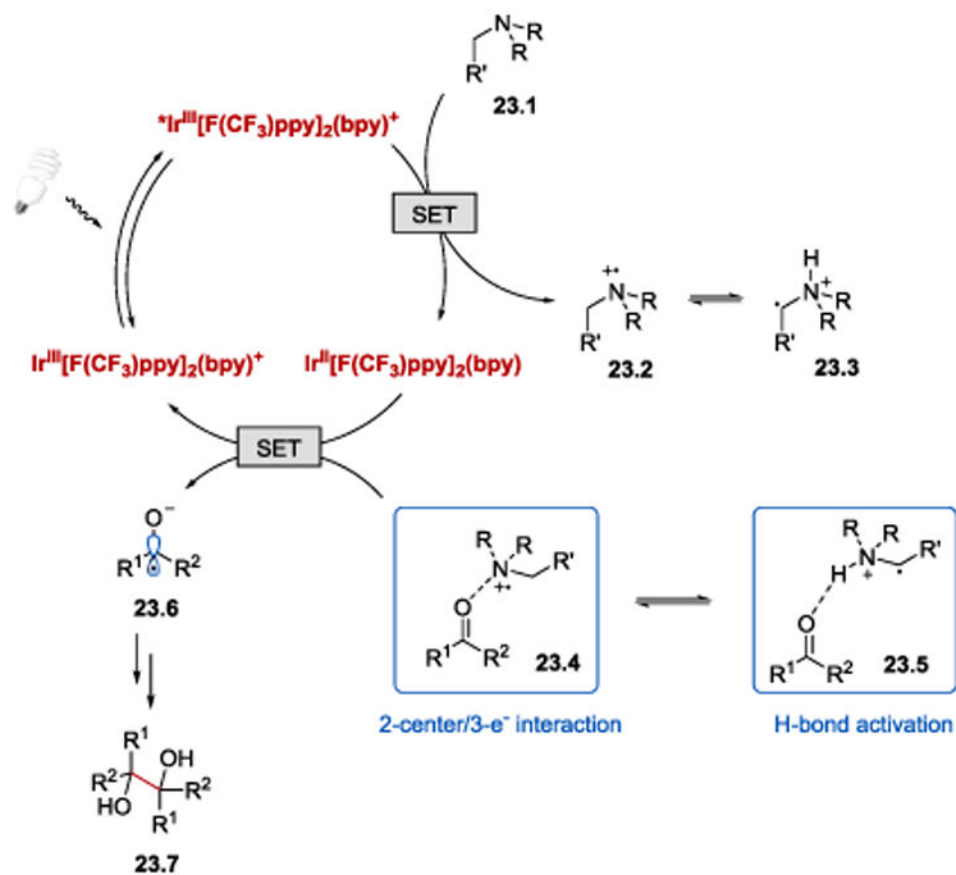
**Scheme 21.**

Photoredox-catalysed pinacol coupling of aldehydes and ketones. <sup>a</sup>1.5 equiv of NBu<sub>3</sub> was used.<sup>56</sup>

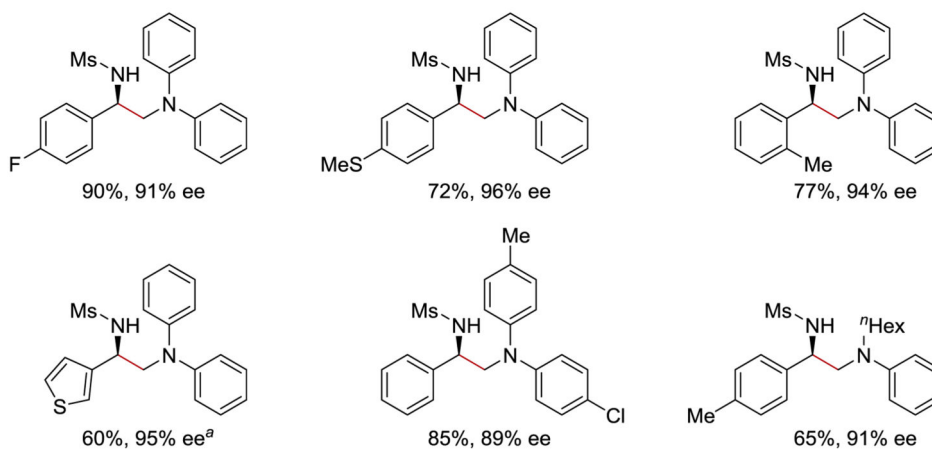
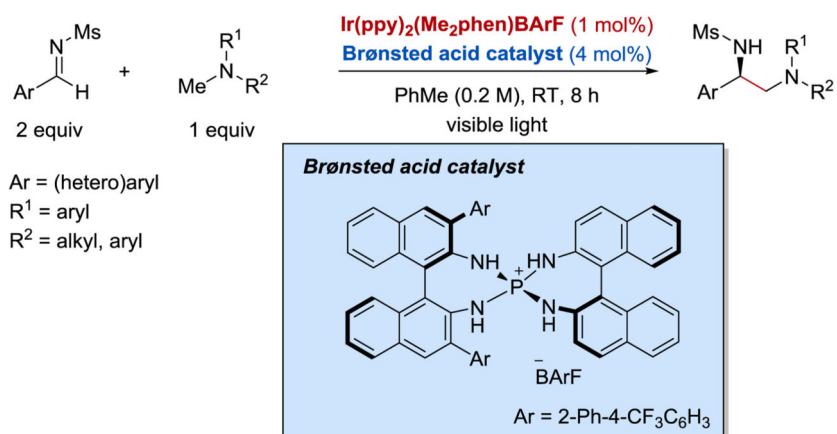




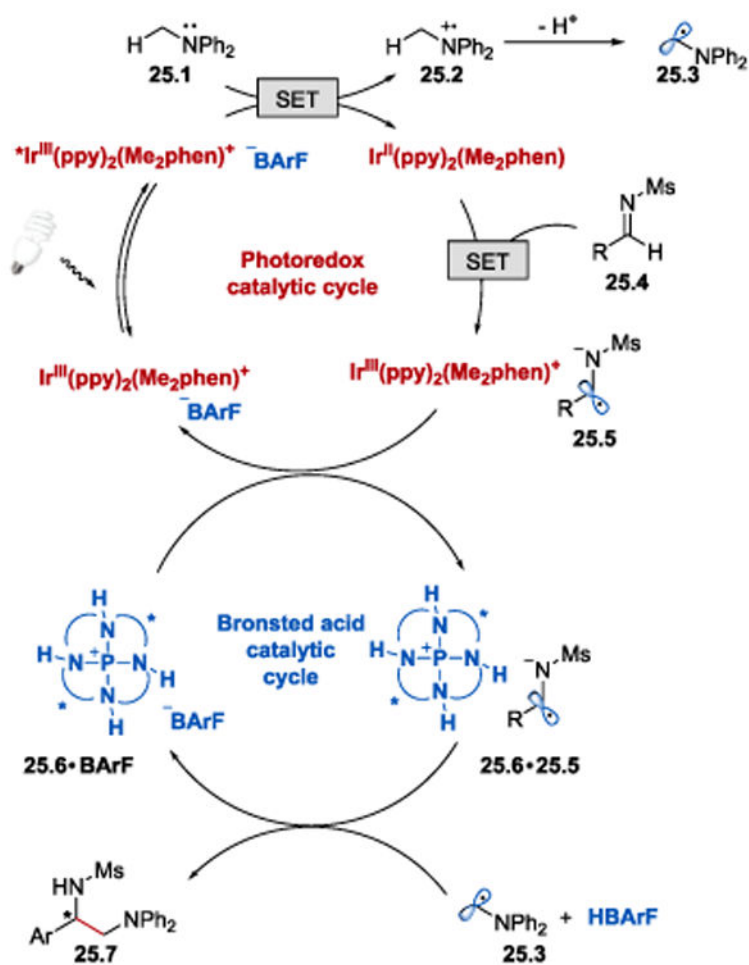
**Scheme 22.**  
Photoredox-catalysed imino-pinacol coupling.<sup>56</sup>



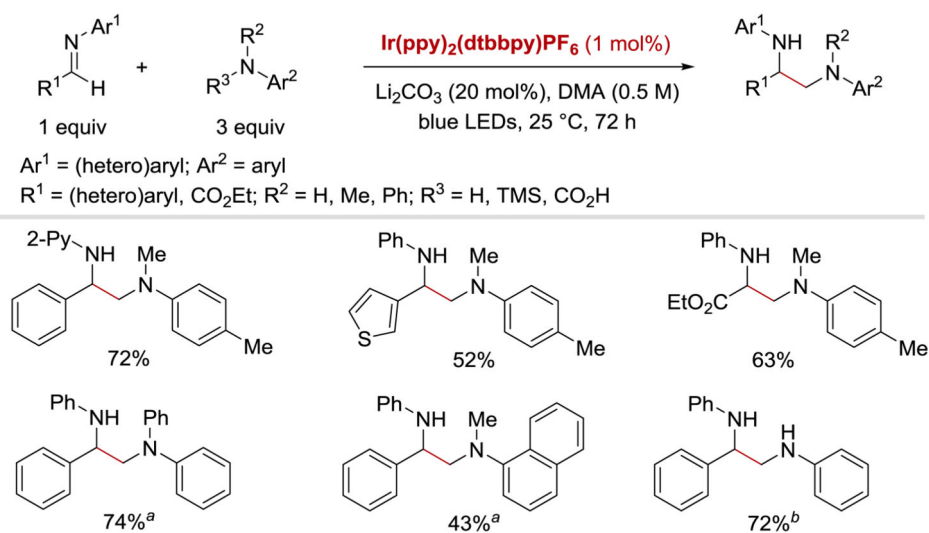
**Scheme 23.** Postulated catalytic cycle for the photoredox-catalysed pinacol coupling of aldehydes and ketones.<sup>56</sup>

**Scheme 24.**

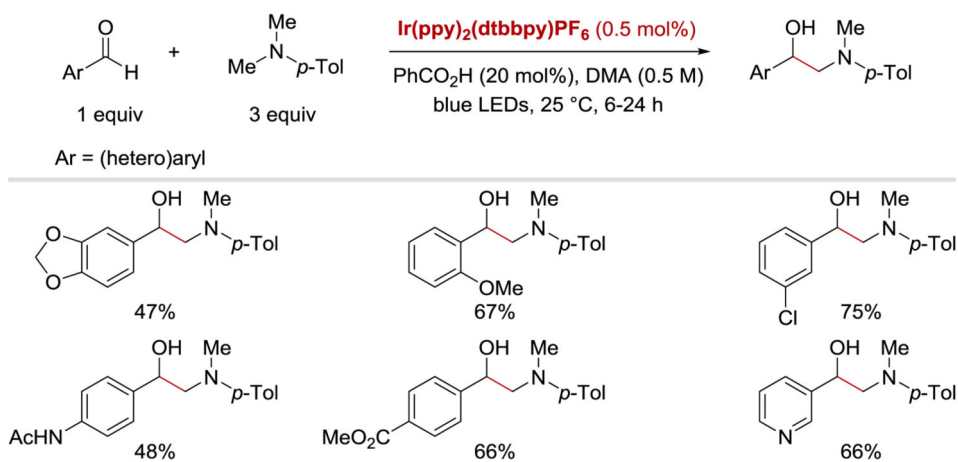
Asymmetric  $\alpha$ -coupling of imines with *N*-arylamino methanes under synergistic chiral Brønsted acid/photoredox catalysis. <sup>a</sup>0.05 M, 34 h.<sup>64</sup>



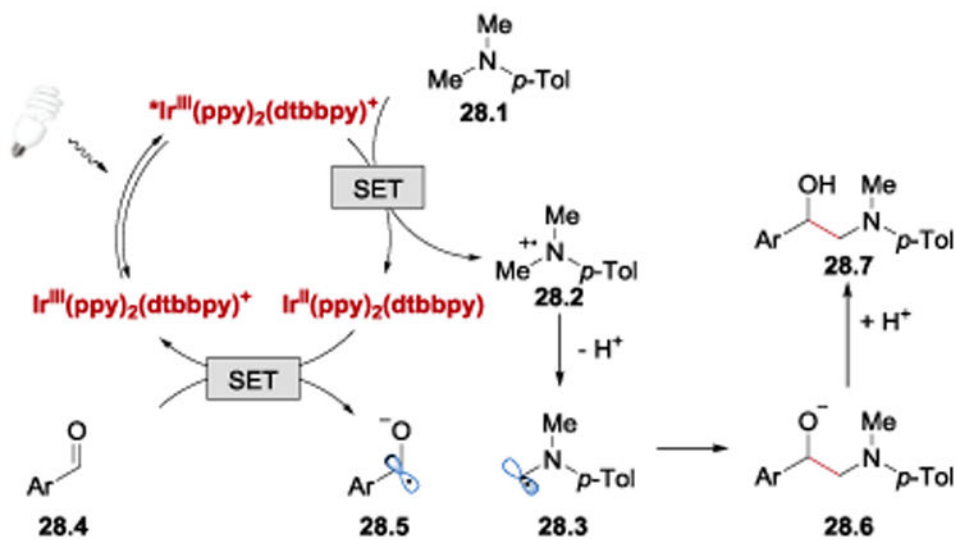
**Scheme 25.** Proposed mechanism of asymmetric  $\alpha$ -coupling of imines with *N*-arylaminoethanes.<sup>64</sup>

**Scheme 26.**

$\alpha$ -Coupling of imines with anilines. <sup>a</sup>R<sup>3</sup> = H <sup>b</sup>R<sup>3</sup> = TMS<sup>58</sup>



**Scheme 27.**  
Coupling of aldehydes with *N,N*-dimethyl-*p*-toluidine.<sup>58</sup>

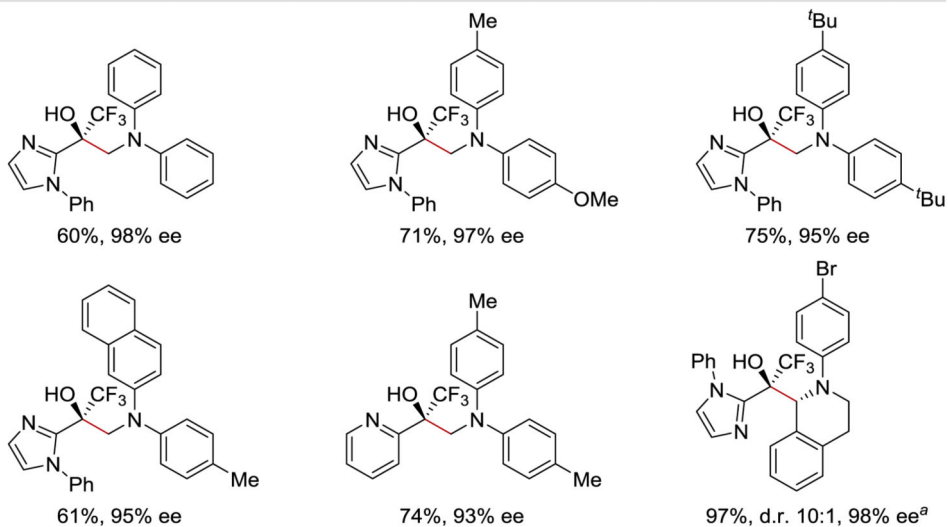
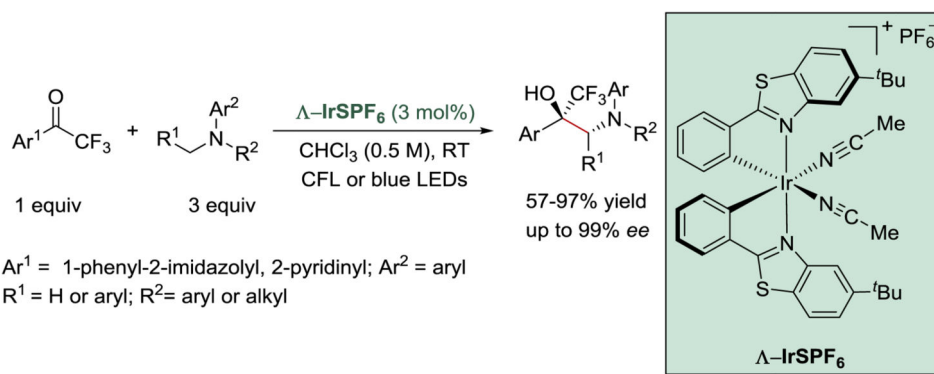


Scheme 28.

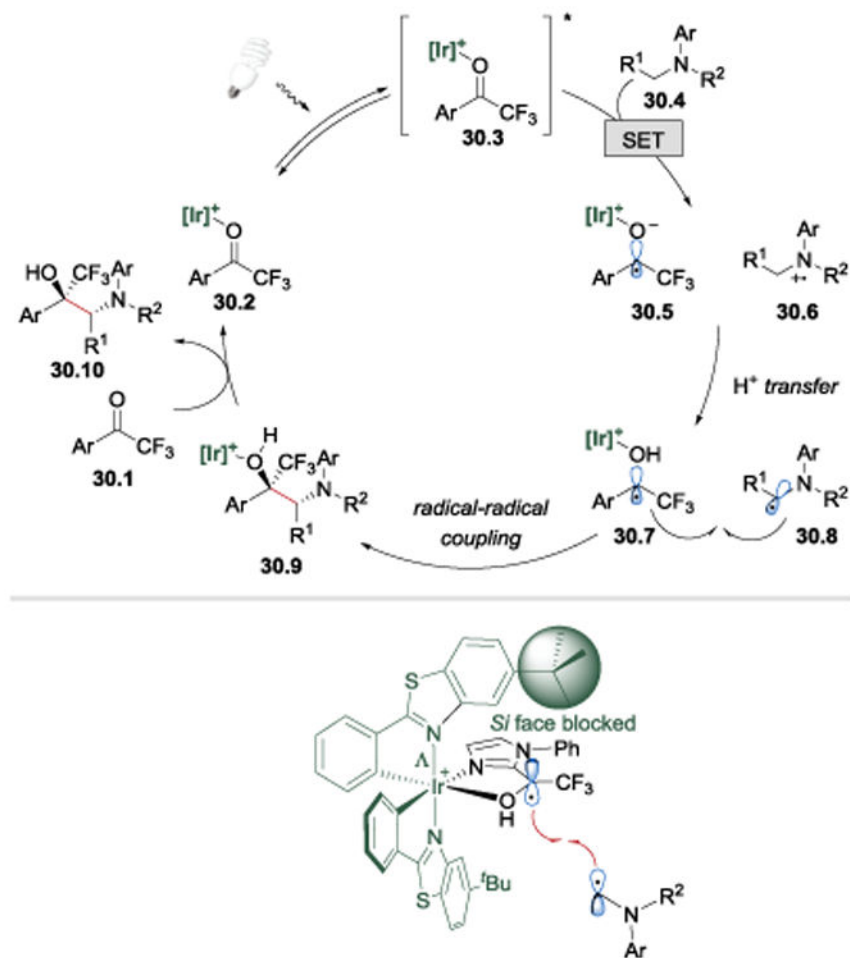
Proposed photoredox catalytic cycle for the synthesis of unsymmetrical 1,2-aminoalcohols.

58

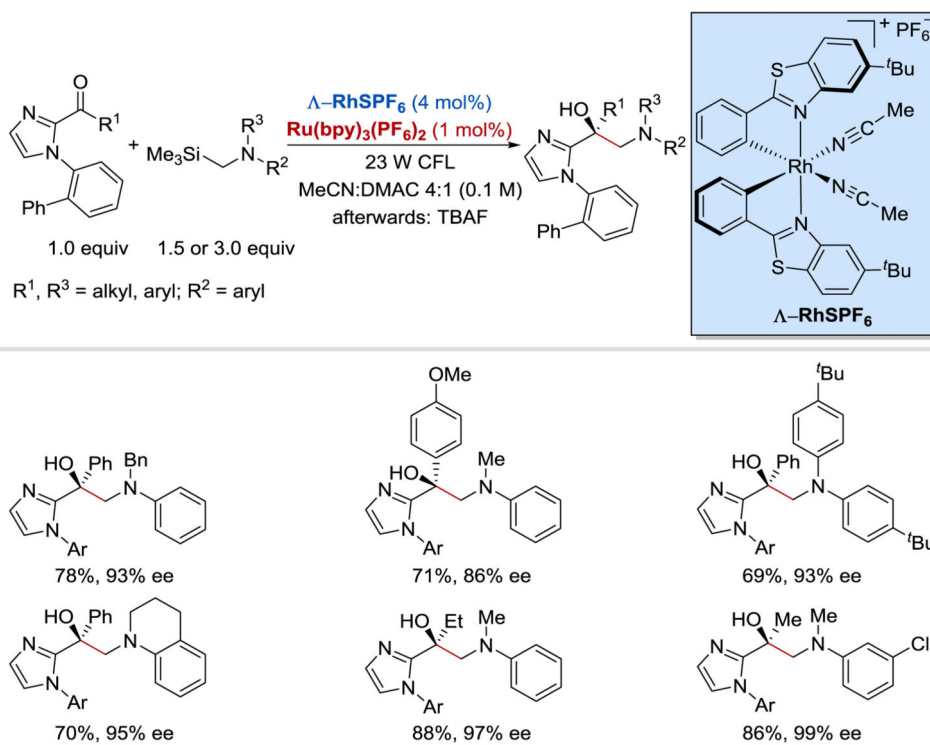


**Scheme 29.**

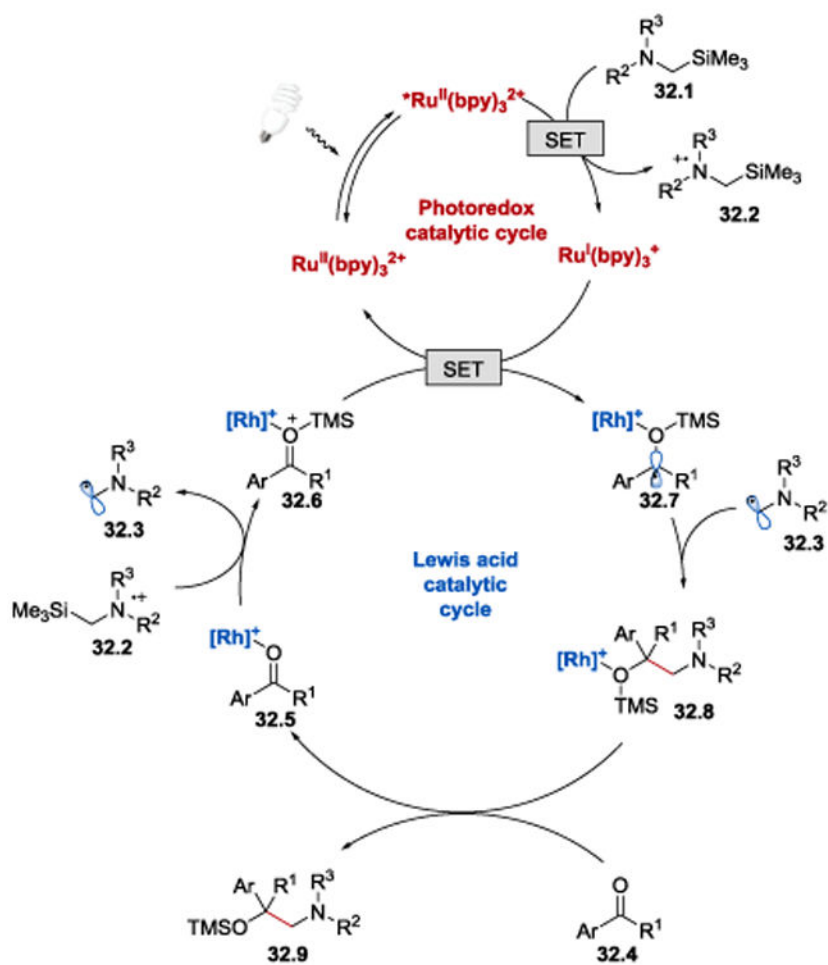
Photoredox-catalysed enantio- and diastereoselective synthesis of 1,2-amino alcohols.<sup>45</sup> mol% of  $\Delta\text{-IrS}$  was used.<sup>62</sup>

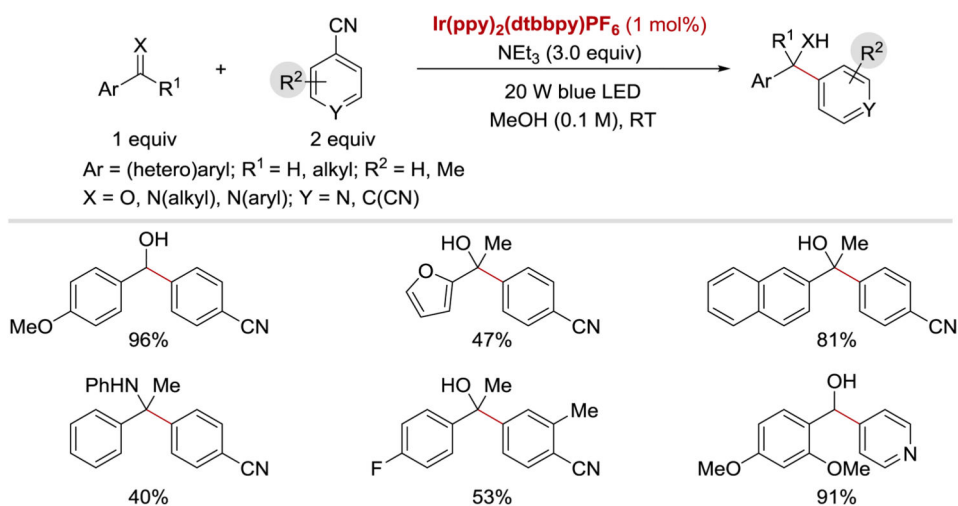


**Scheme 30.** Postulated mechanism for the visible-light-activated catalytic asymmetric process and a proposed stereochemical model for the asymmetric induction.<sup>62</sup>

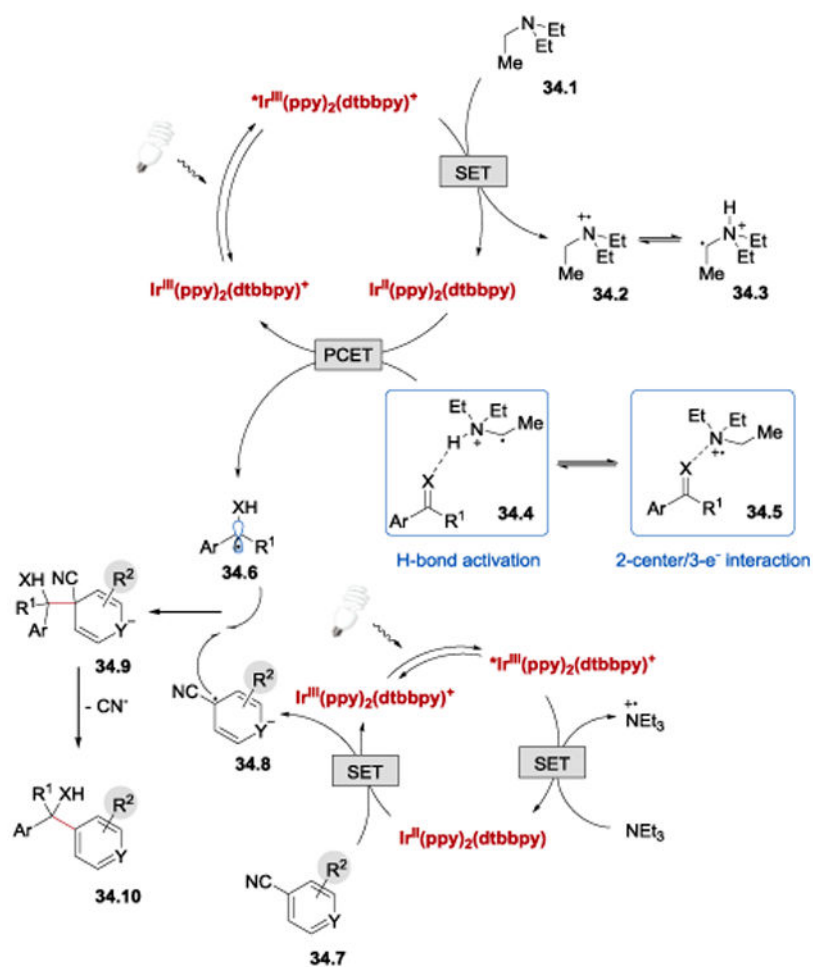


**Scheme 31.** Enantioselective synthesis of 1,2-aminoalcohols under Rh/Ru photoredox catalysis.<sup>97</sup>

**Scheme 32.**Proposed mechanism of the visible-light activated Rh/Ru dual catalysis.<sup>97</sup>

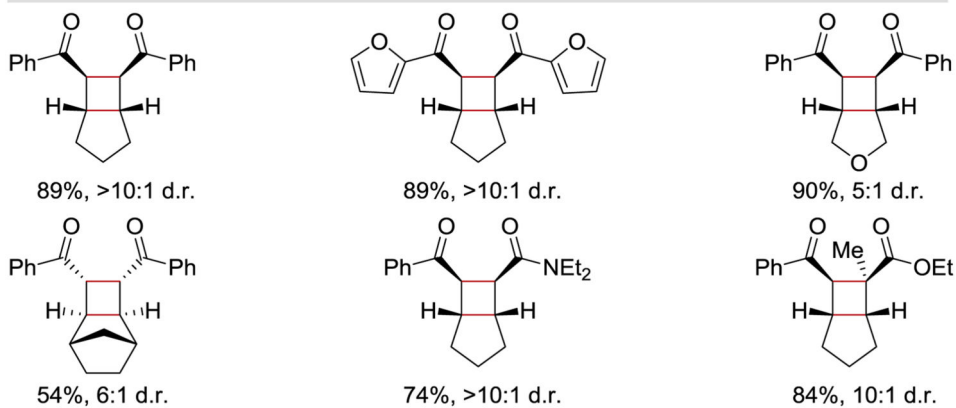
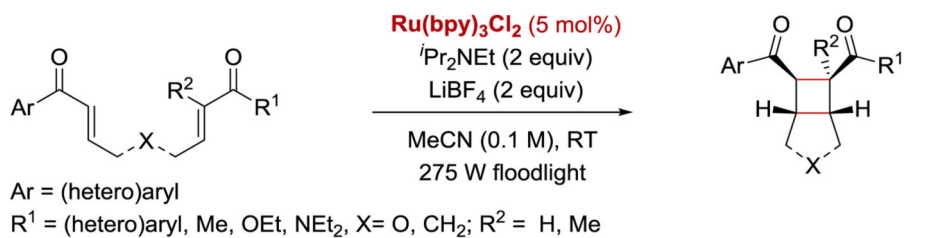


**Scheme 33.**  
Photocatalytic arylation of aldehydes and imines.<sup>99</sup>



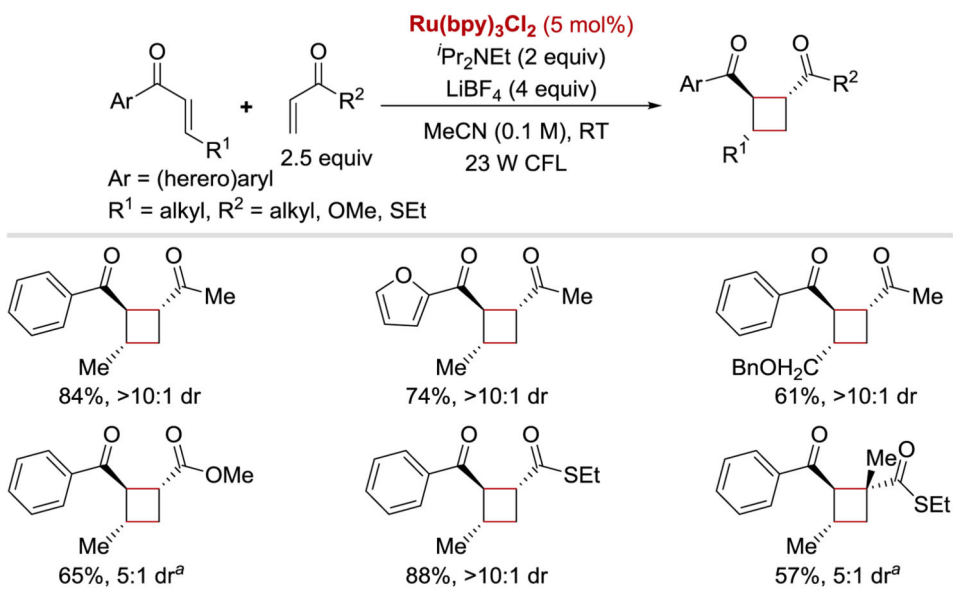
Scheme 34.

Proposed mechanism for the photocatalytic arylation of aldehydes and imines.<sup>99</sup>

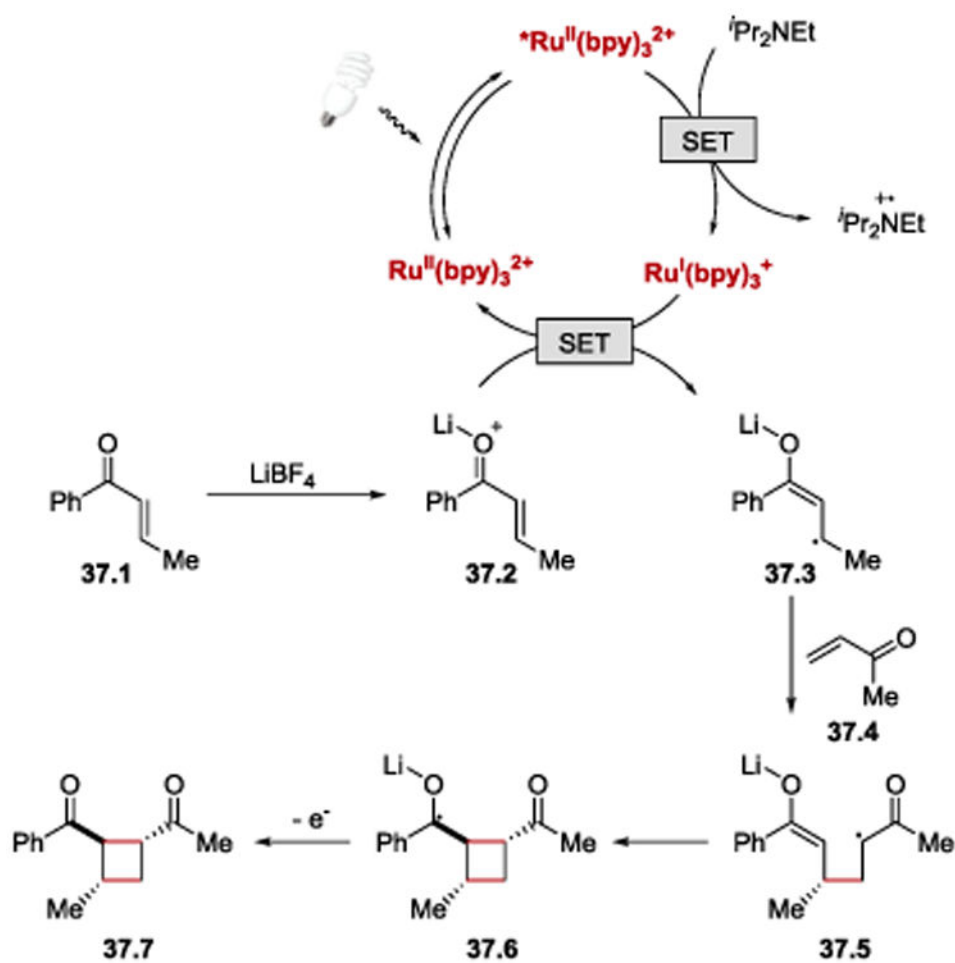


**Scheme 35.**  
Photocatalytic [2+2] enone cycloaddition.<sup>47</sup>

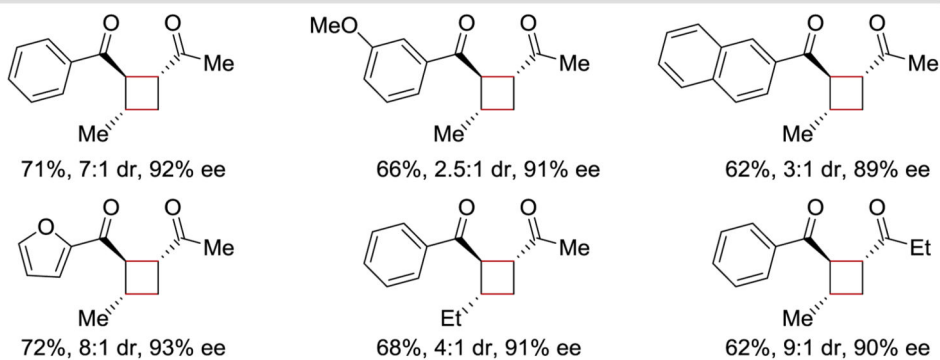
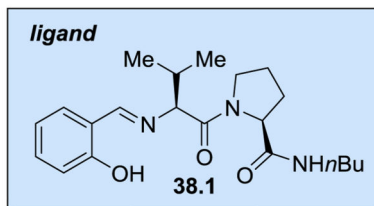
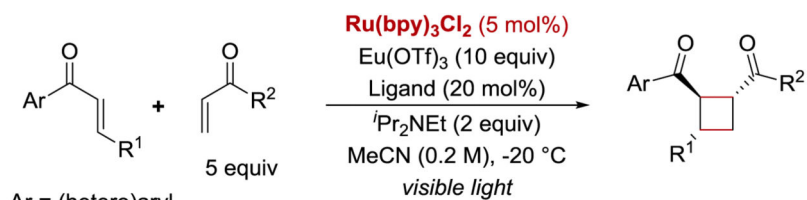


**Scheme 36.**

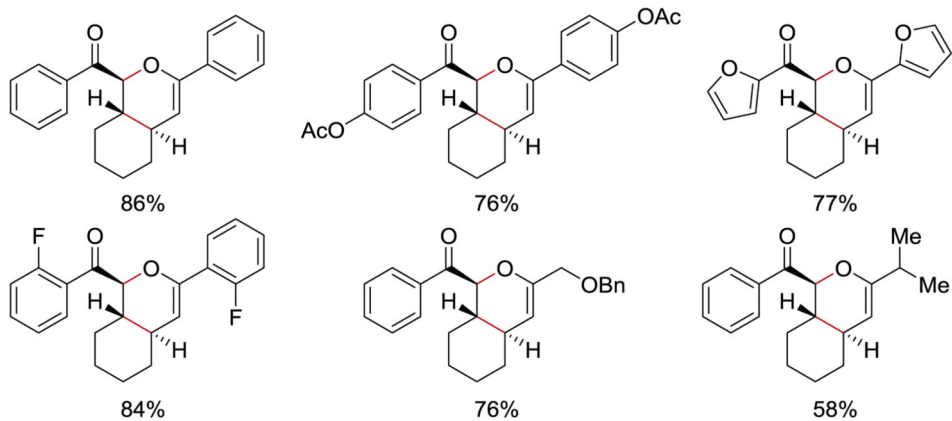
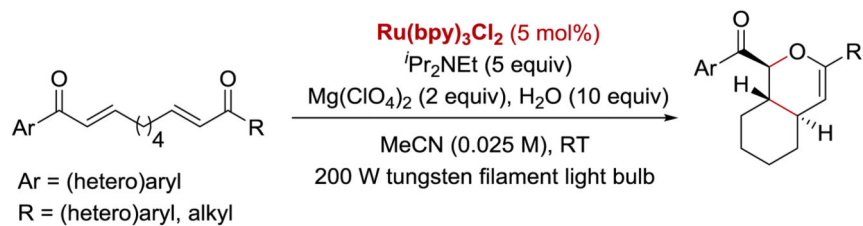
Photocatalytic intermolecular [2+2] enone cycloaddition. <sup>a</sup>Reaction was performed with 6 equiv of Michael acceptor.<sup>48</sup>



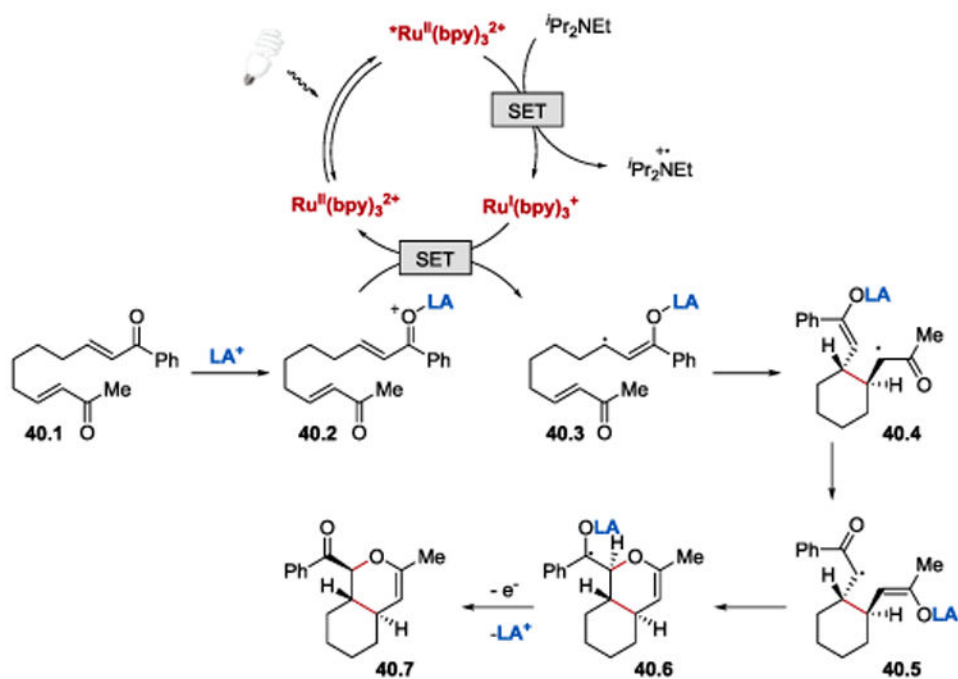
**Scheme 37.**  
Proposed mechanism of photocatalytic [2+2] enone cycloaddition.<sup>100</sup>



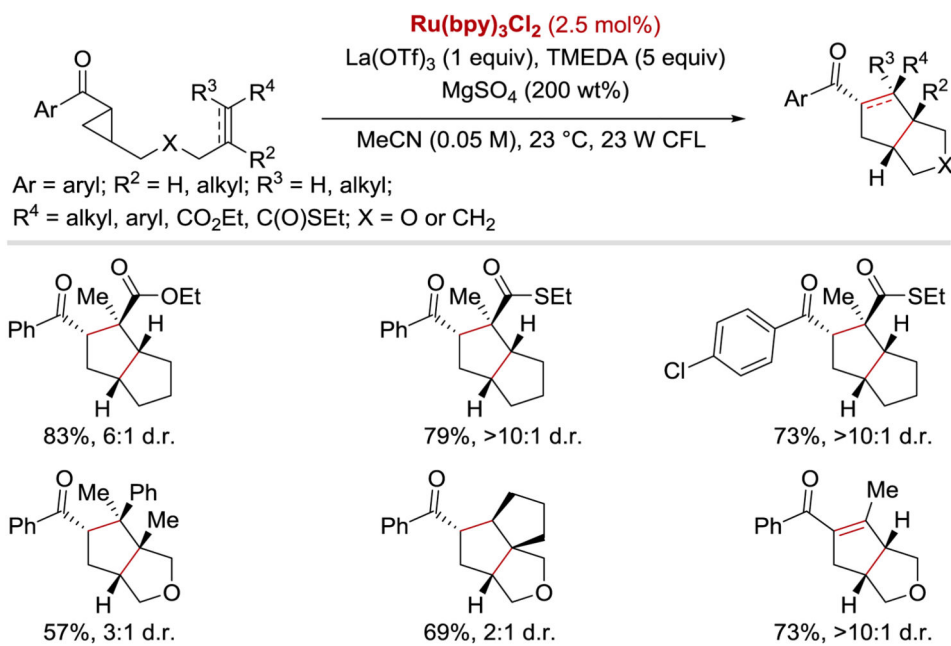
**Scheme 38.** Photocatalytic enantioselective intermolecular [2+2] enone cycloaddition.<sup>55</sup>

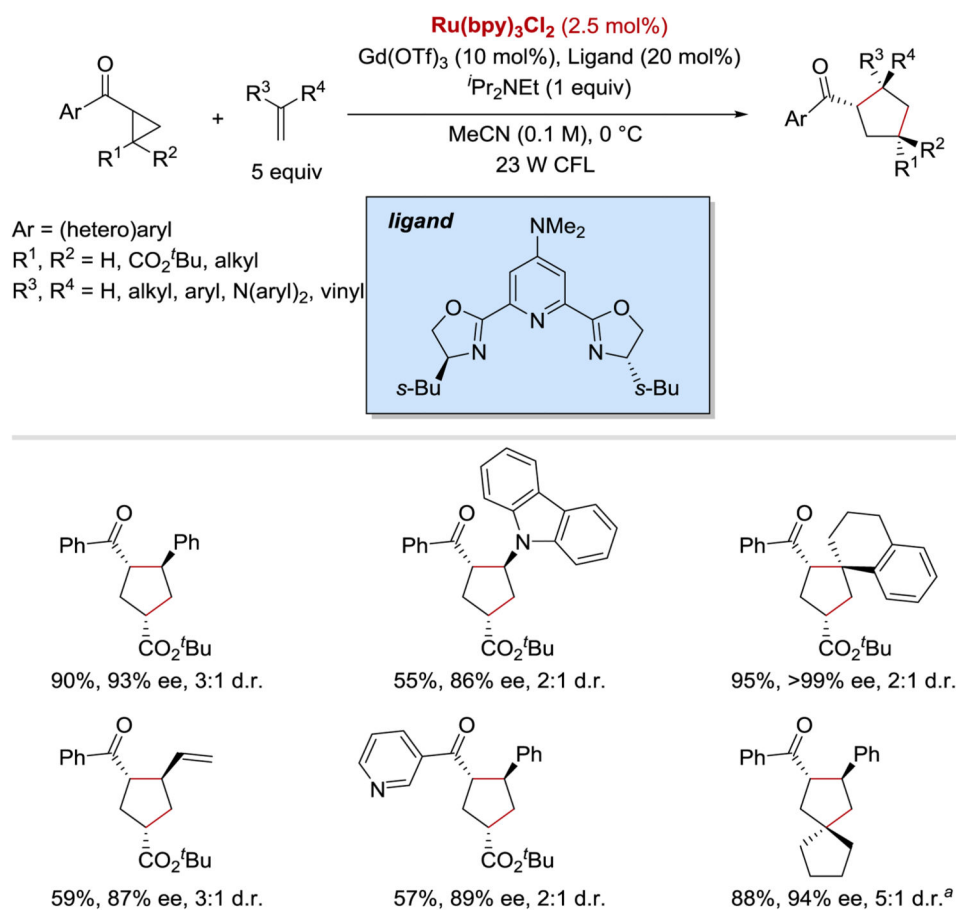


**Scheme 39.**  
Photocatalytic [4+2] cycloaddition.<sup>50</sup>

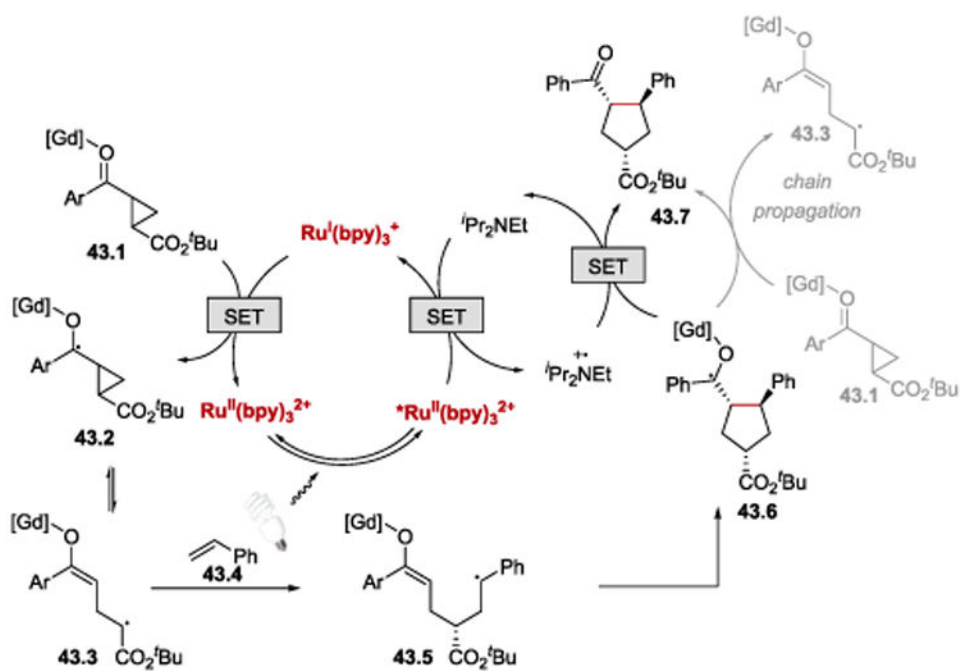
**Scheme 40.**

Proposed mechanism of the regioselective [4+2] hetero Diels-Alder cycloaddition reaction.  
50

**Scheme 41.**Photocatalytic [3+2] cycloaddition of aryl cyclopropyl ketones.<sup>102</sup>

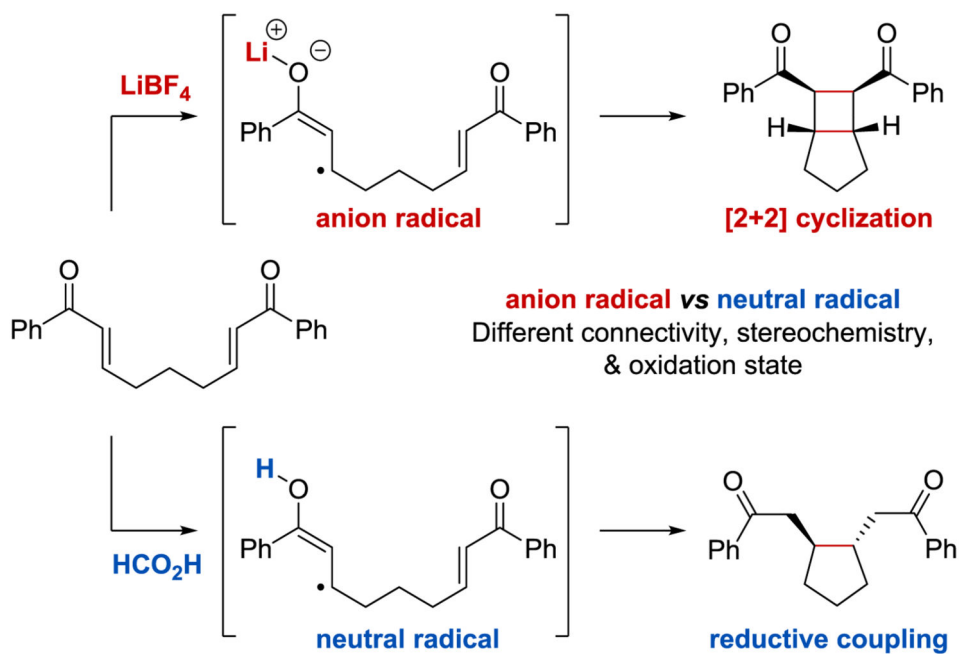
**Scheme 42.**

Photocatalytic enantioselective intermolecular [3+2] cycloaddition. <sup>a</sup>Reaction conducted using 20 mol% Gd(OTf)<sub>3</sub> and 30 mol% of the ligand at -20 °C.<sup>57</sup>

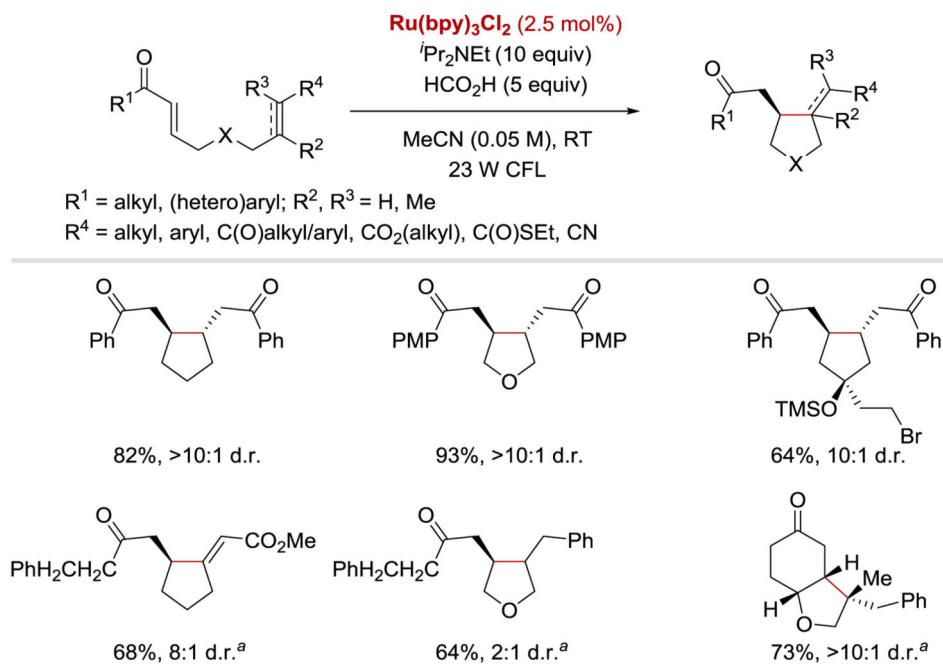


**Scheme 43.**  
Proposed mechanism for enantioselective [3+2] cycloaddition.<sup>57</sup>

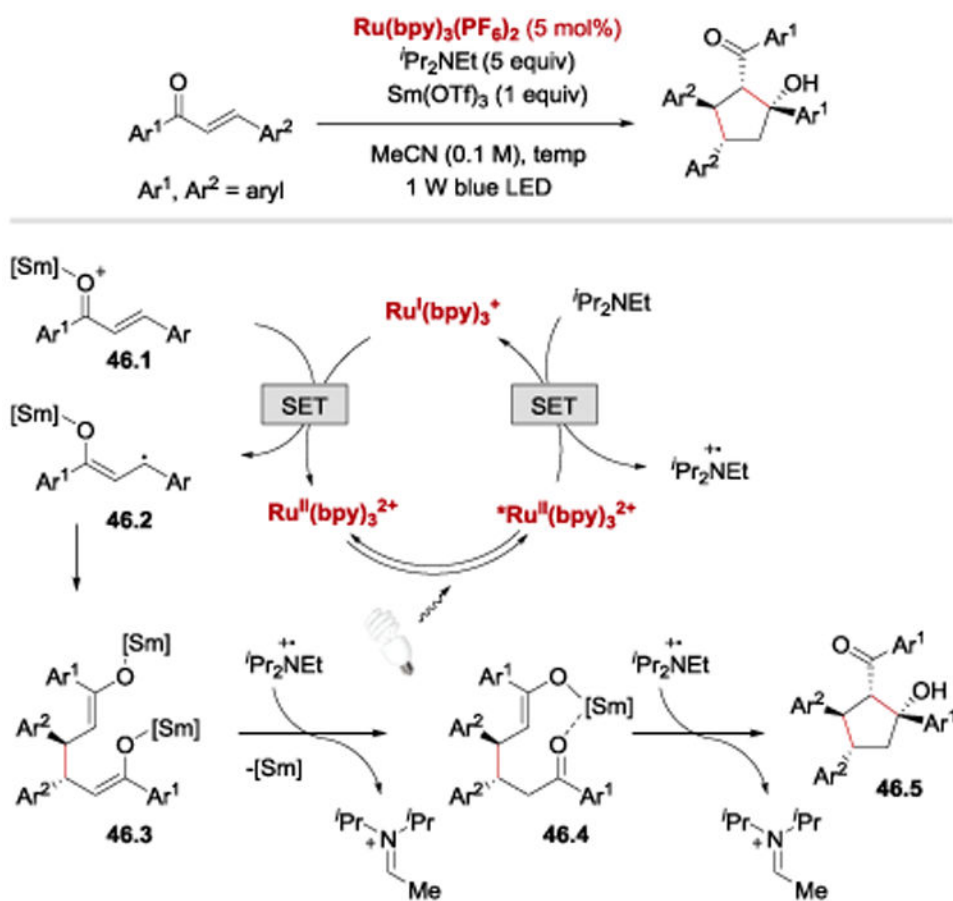




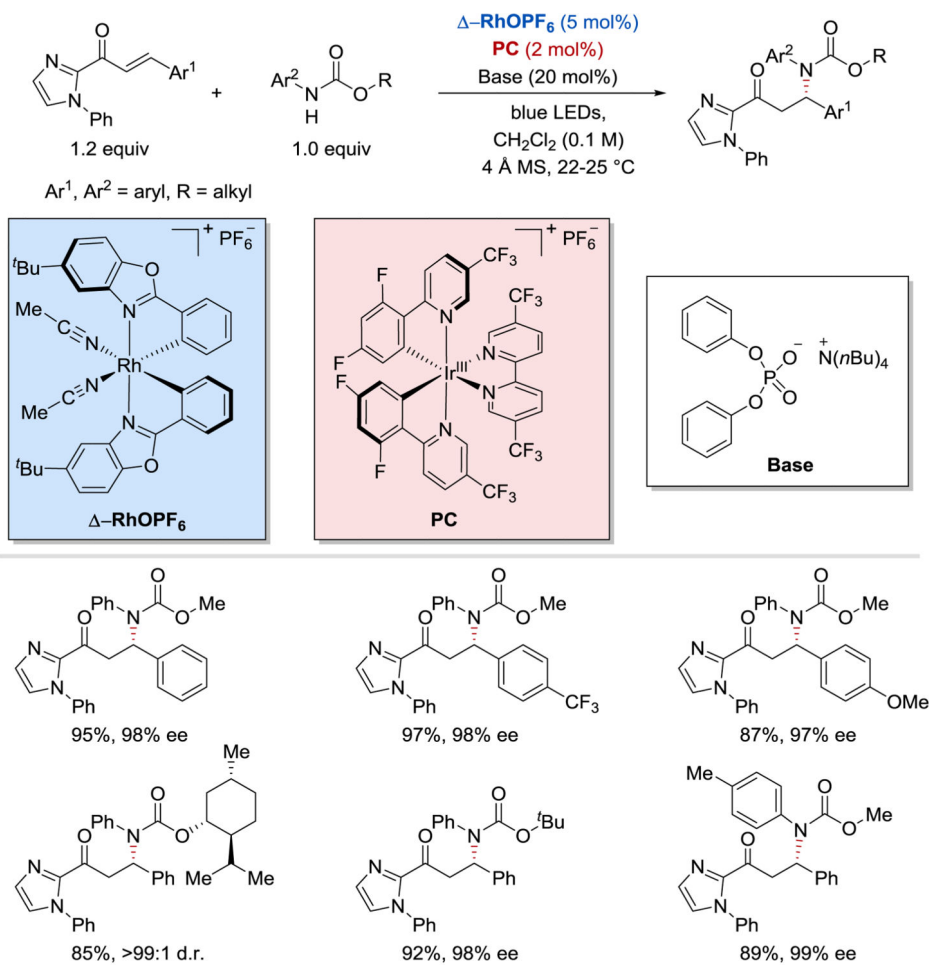
**Scheme 44.** Divergent reactivity of photoredox-generated radical and anion radical intermediates.<sup>49</sup>

**Scheme 45.**

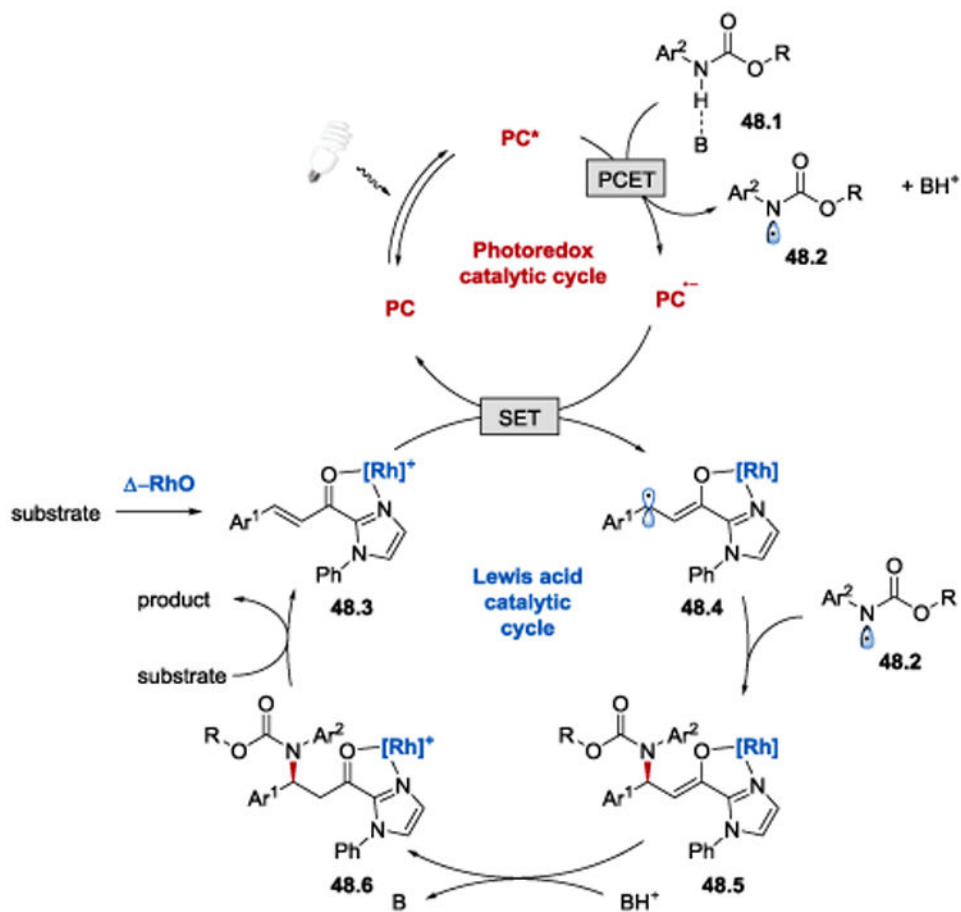
Photocatalytic reductive cyclization of enones. <sup>a</sup>Reaction was conducted with 2.5 mol% of Ir(ppy)<sub>2</sub>(dtbbpy)(PF<sub>6</sub>).<sup>49</sup>



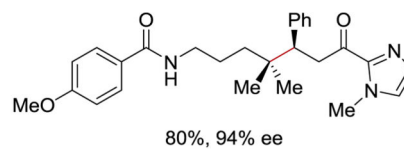
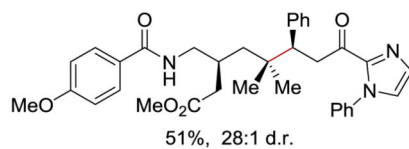
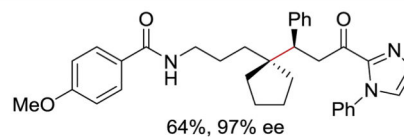
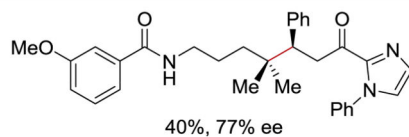
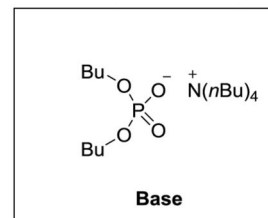
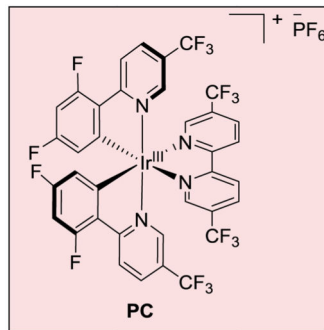
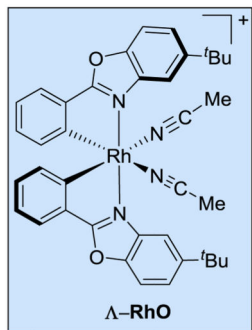
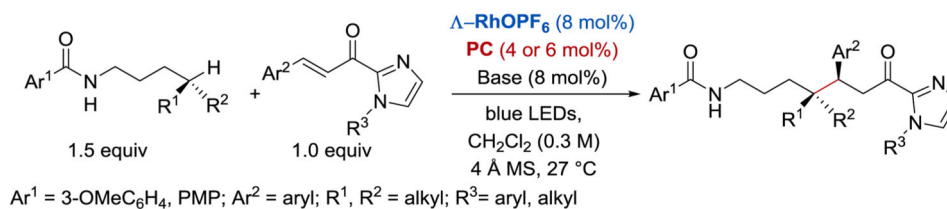
**Scheme 46.**  
 Reductive chalcone dimerization under photoredox conditions.<sup>103</sup>



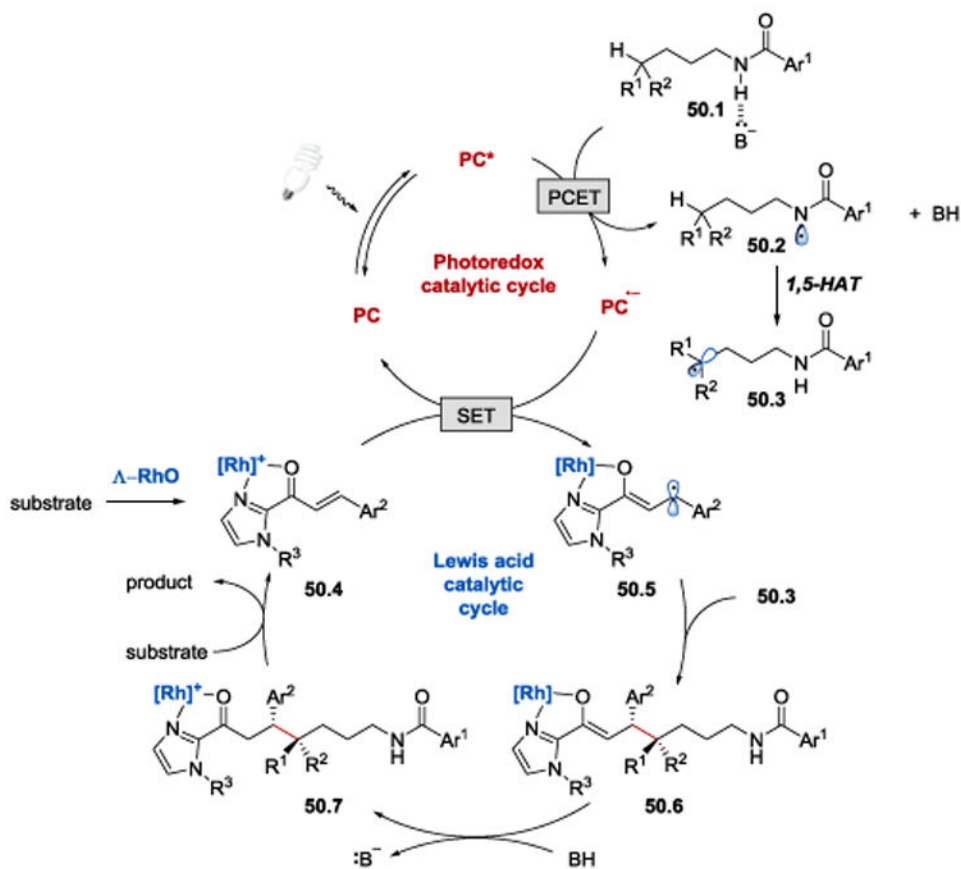
**Scheme 47.**  
 Enantioselective  $\beta$ -amination of enones.<sup>104</sup>



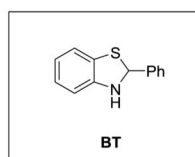
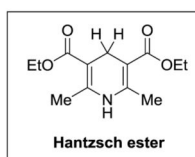
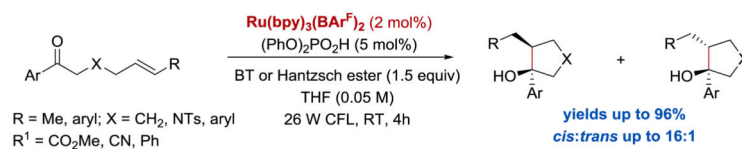
**Scheme 48.**  
Proposed mechanism of enantioselective  $\beta$ -amination of enones.<sup>104</sup>

**Scheme 49.**

Asymmetric  $\delta$ -functionalization of *N*-alkyl amides under photoredox conditions.<sup>105</sup>



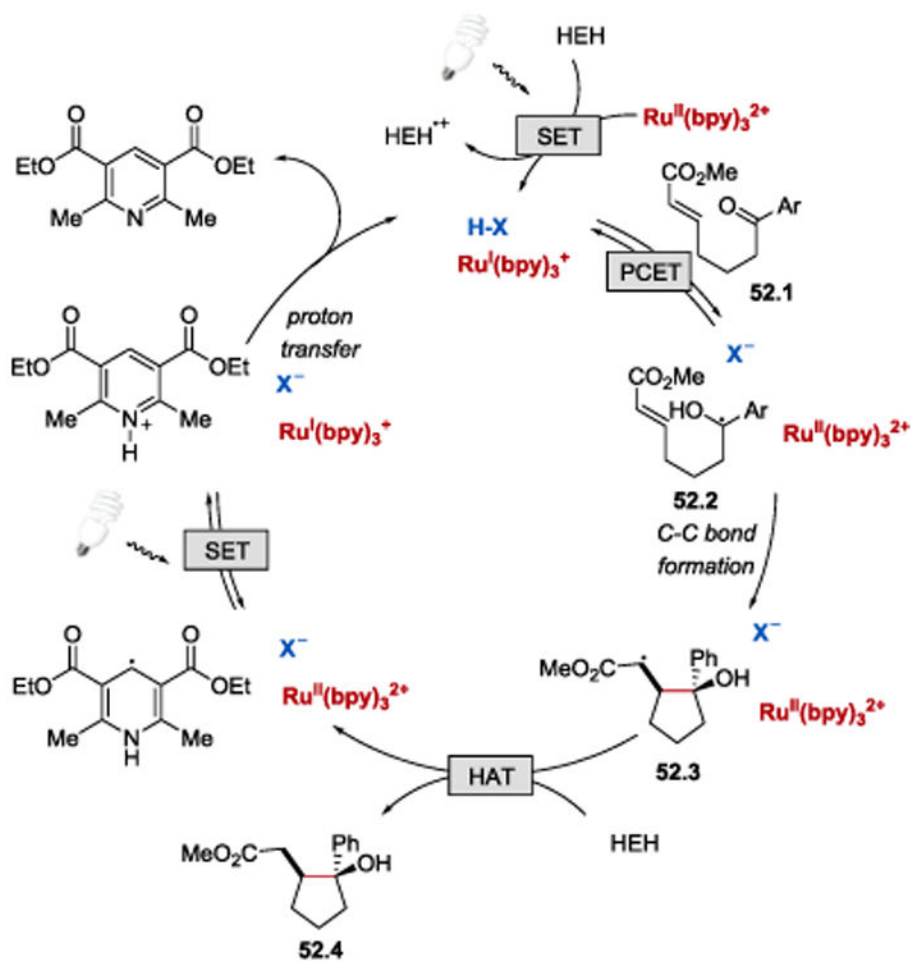
**Scheme 50.** Proposed mechanism of asymmetric  $\delta$ -functionalization of *N*-alkyl amides under photoredox conditions.<sup>104</sup>



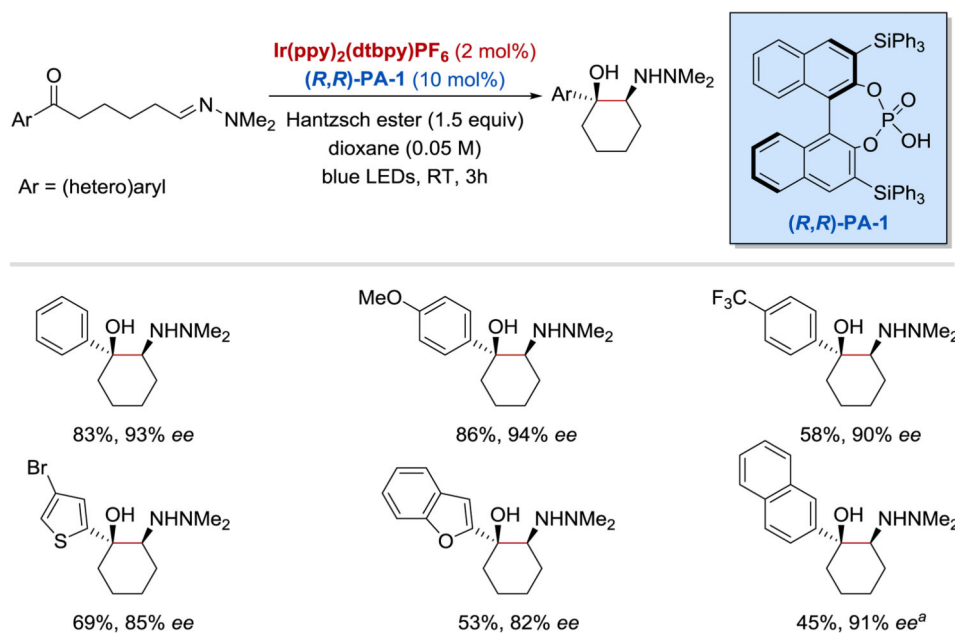
Substrate	Products	Yield (cis:trans)
		73% 11:1
		80% 3.4:1
		64% 10:1
		78% 1.2:1
		68%

**Scheme 51.**  
Photoredox-catalyzed intramolecular ketyl-olefin coupling reaction.<sup>54</sup>

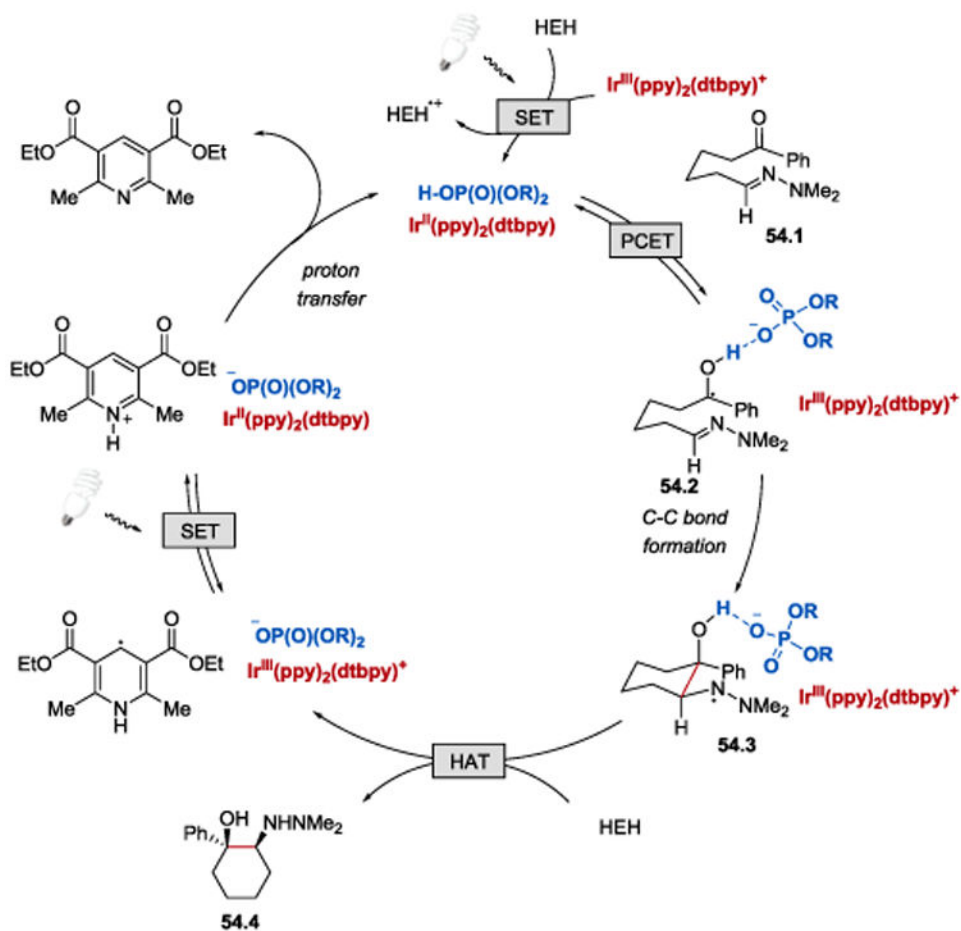




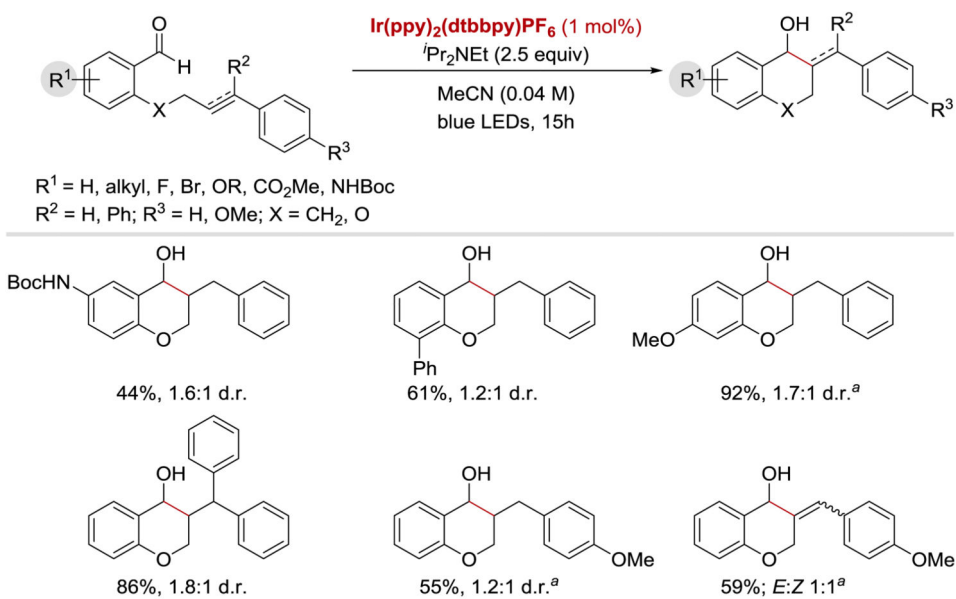
**Scheme 52.**  
Proposed mechanism for photoredox-catalysed intramolecular ketyl-olefin coupling reaction.<sup>54</sup>

**Scheme 53.**

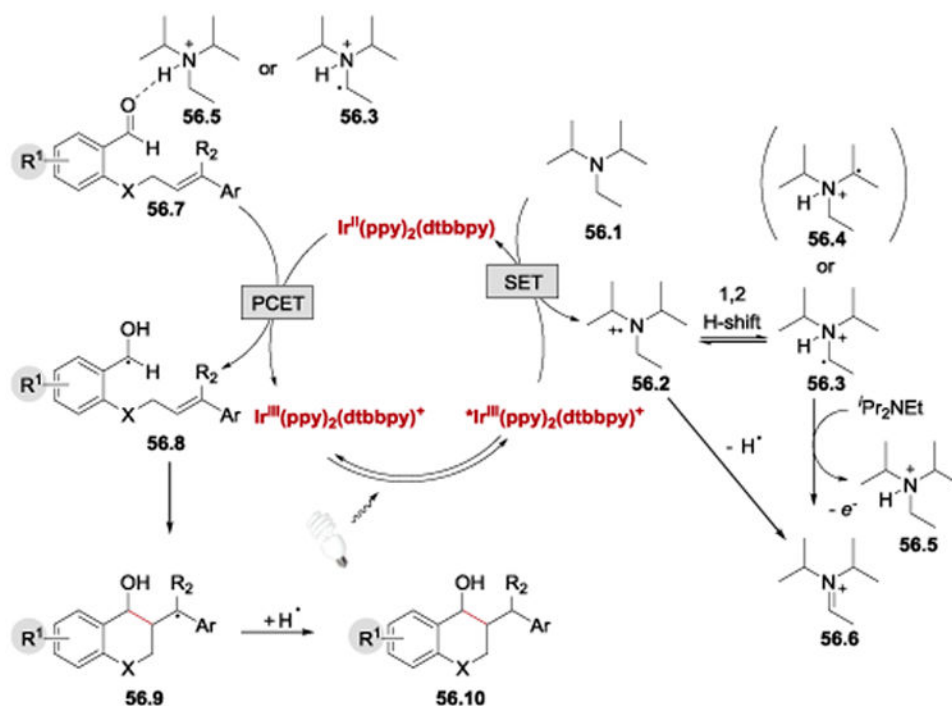
Photoredox-catalysed asymmetric intramolecular aza-pinacol coupling reaction. <sup>a</sup>Reaction run at 0 °C in THF.<sup>53</sup>

**Scheme 54.**

Proposed mechanism for the photoredox-catalysed asymmetric intramolecular aza-pinacol coupling reaction.<sup>53</sup>

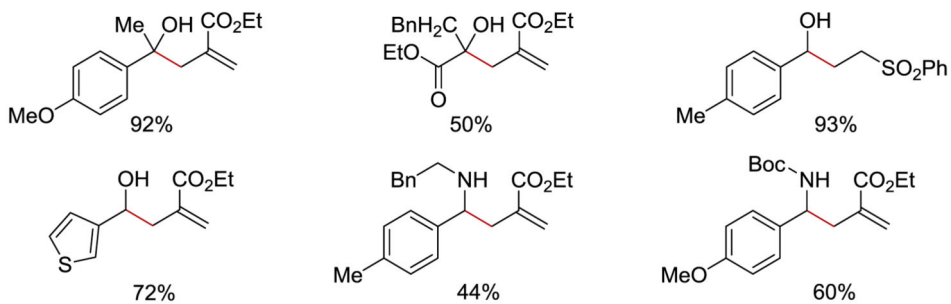
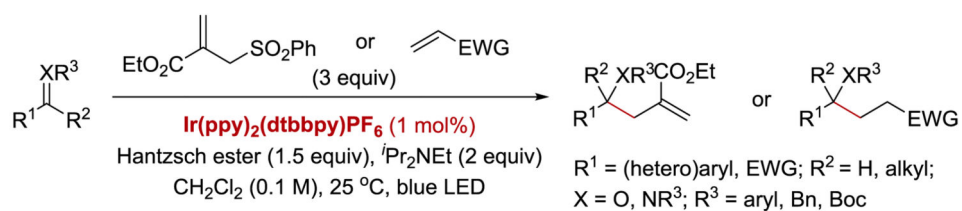
**Scheme 55.**

Intramolecular photoredox-catalysed ketyl-alkene/alkyne coupling. <sup>a</sup>Reaction performed with 2.5 mol% of photocatalyst.<sup>59</sup>

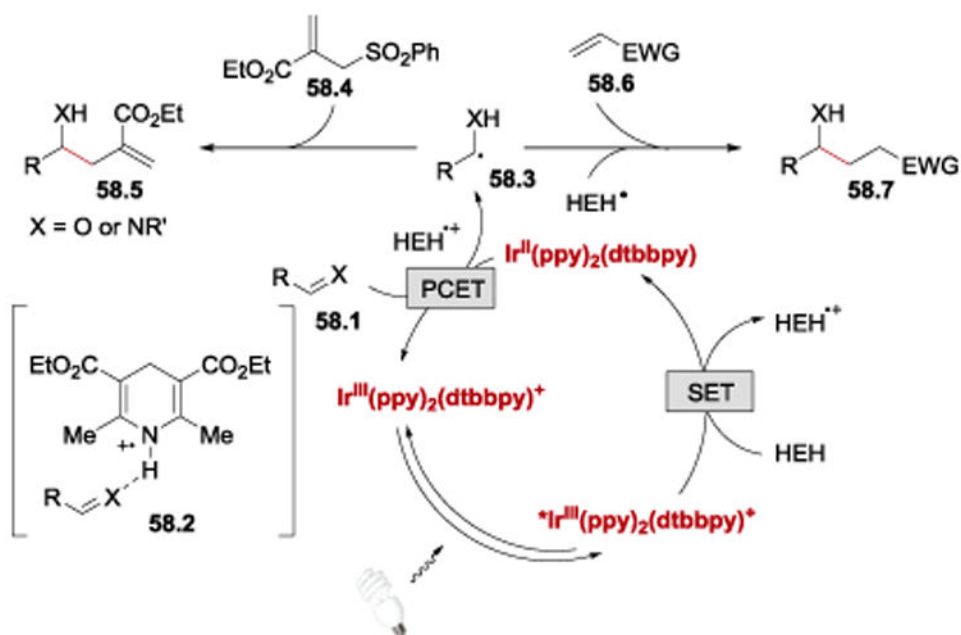


**Scheme 56.**

Proposed reaction mechanism of the photoredox-catalysed intramolecular ketyl-olefin/alkyne coupling.<sup>59</sup>

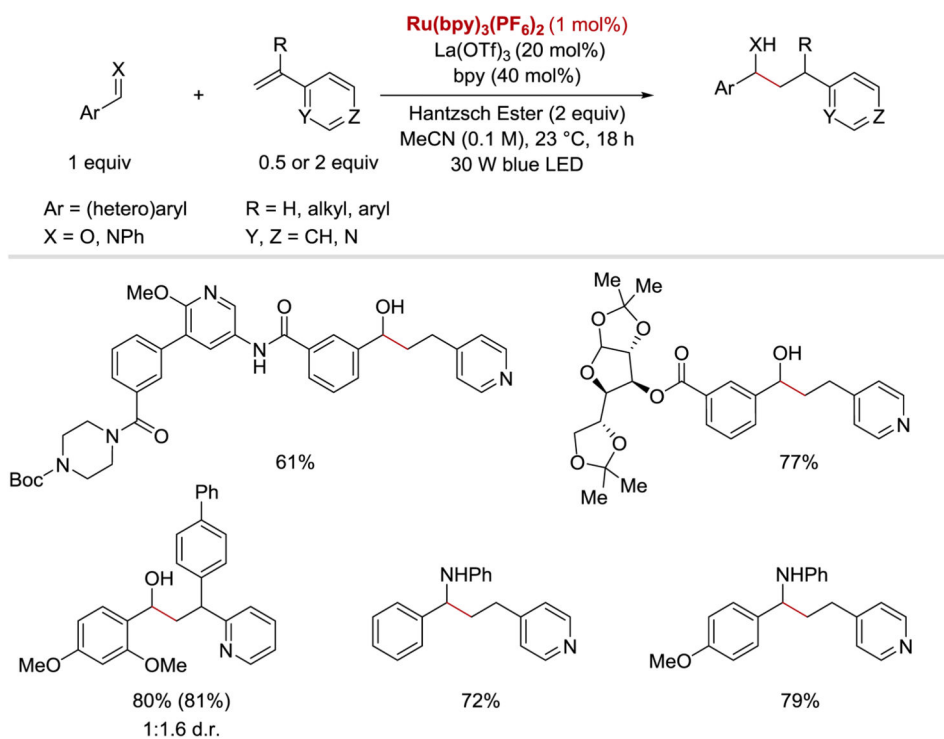
**Scheme 57.**

Allylation reaction of aldehydes, ketones and imines under photoredox conditions.<sup>60</sup>



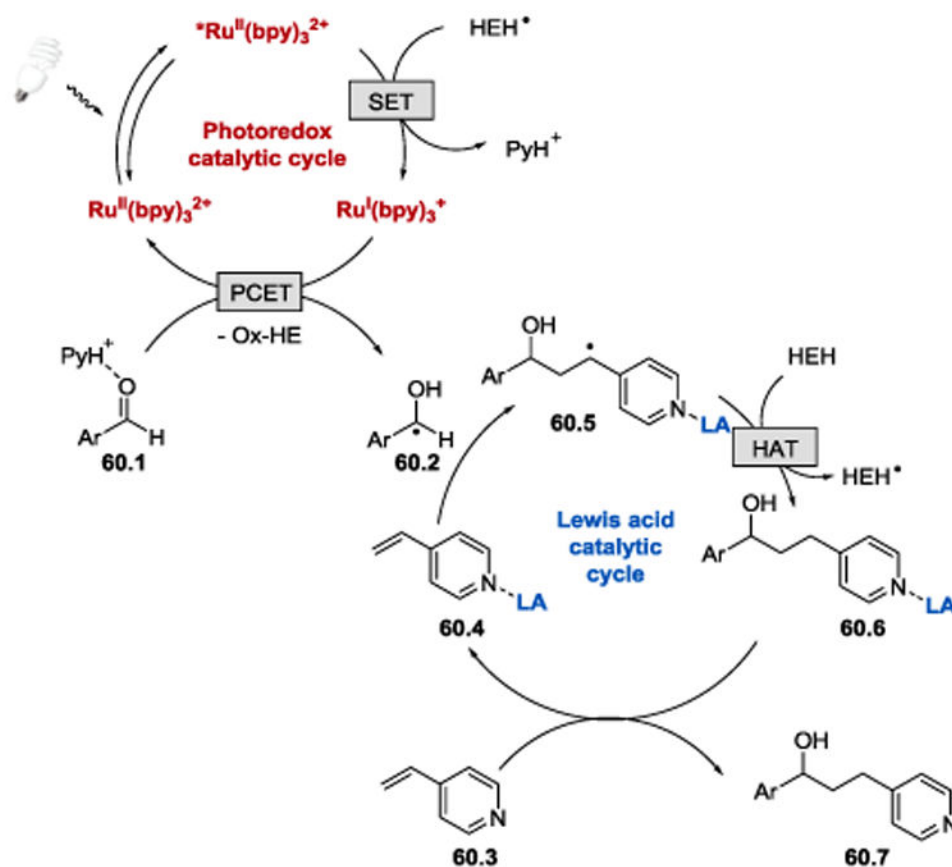
Scheme 58.

Proposed mechanism of the allylation and Michael addition reactions.<sup>60</sup>

**Scheme 59.**

Photoredox-catalysed coupling reaction between aldehydes/imines and 4-vinylpyridine.  $^1\text{H}$  NMR yields are provided in parenthesis.<sup>107</sup>



**Scheme 60.**

Proposed reaction mechanism of the photoredox coupling reaction between aldehydes and alkenylpyridines.<sup>107</sup>